JAHRBUCH DER GEOLOGISCHEN BUNDESANSTALT

Jb. Geol. B.-A. | ISSN 0016-7800 | Band 137 | Heft 1 | S. 197-212 | Wien, Juni 1994

Microstructural Evolution of Metapelites from the Austroalpine Basement North of Staller Sattel During Pre-Alpine and Alpine Deformation and Metamorphism (Eastern Tyrol, Austria)

By BERNHARD SCHULZ *)

With 9 Text-Figures and 1 Table

Osttirol
Ostalpin
Varisziden
Basement
Metapelite
Metamorphose
Deformation
Mikrogefüge
Quarzgefüge
Scherzone

Österreichische Karte 1 : 50.000
Blatt 177

Contents

Mikrogefügeentwicklung von Metapeliten des Ostalpinen Grundgebirges nördlich des Staller Sattels während der voralpidischen und alpidischen Deformation und Metamoprphose (Osttirol, Österreich)

Zusammenfassung

Metapelite des ostalpinen Altkristallins zwischen Defereggen-Antholz-Vals-Linie und Rieserferner-Tonalit nördlich des Staller Sattels zeigen eine mehrphasige Deformations- und Metamorphosegeschichte. In Glimmerschiefern wuchsen Granat-führende Paragenesen während der Ausbildung der Foliationen S_1 und S_2 durch progressive Deformation D_1-D_2. Die stark zonierten Granate koexistierten mit Glimmern und teilweise albitischem Plagioklas. Dies ermöglichte, eine frühe prograde prä/syn-S_2-Metamorphose mit einem Hochdruckstadium (650°C/15 kbar) und einem anschließenden hochtemperierten amphibolitfaziellen Stadium (680°C/7 kbar) mittels Kationen-Austausch- und -Transfer-Geothermobarometrie zu rekonstruieren. Diskordant S_2 durchschlagende spätvariskische Pegmatite, parallele linear-planare D_1-D_2-Strukturen in oberordovizischen Granitoiden und deren Nebengesteinen sowie ähnliche Granat-Zonierungstrends in Glimmerschiefern aus angrenzenden Regionen mit spätvariskischen Glimmer-Abkühlaltern, deuten ein frühvariskisches Alter dieser Metamorphose an. Die Pegmatite und die älteren Strukturen wurden von einer vermutlich frühalpidischen Foliation S_{A1} aus feinkörnigem Muscovit unter grünschieferfaziellen Bedingungen (450°C/3–4 kbar) überprägt. Eine feinkörnige Rekristallisation von Paragonit sowie eine post-S_2- und post-S_{A1}-Blastese von Andalusit + Staurolith und Sillimanit + Kalifeldspat + Muscovit + Quarz in einigen

*) Author's address: Dr. BERNHARD SCHULZ, Institut für Geologie und Mineralogie, Universität Erlangen-Nürnberg, Schloßgarten 5, D-91054 Erlangen.

Proben lassen sich auf eine spätalpidische Kontaktmetamorphose in der Aureole des 30 Ma alten Rieserferner-Tonalits zurückführen. Die Interpretation dieser Paragenesen in Phasendiagrammen ergab Bedingungen von 620°C/2–3 kbar unmittelbar am Plutonrand. Synkristalline Rotation kontaktmetamorpher Porphyroblasten, monokline Faltung von S_2-S_{A1}-Domänen, eine Foliation S_{A2}, die S_2-S_{A1}-Domänen sigmoidal verformt, und eine Scherband-Foliation S_{A3} sind die Strukturen einer spätalpidischen progressiven Scherzonen-Deformation mit Phyllonitisierung und Mylonitisierung im Nordteil der Defereggen – Antholz – Vals-Linie. In Chlorit-Muscovit-Phylloniten weisen feinkörniger Chlorit + Muscovit + Quarz in S_{A2}, Chlorit + Quarz in S_{A3} und die Quarzgefüge auf sinkende Temperaturen bei dieser Deformation hin. Die entsprechenden kinematischen Kriterien zeigen einheitlich eine sinistrale Seitenverschiebung in der Scherzone an.

Abstract

Metapelites from the Austroalpine basement between the Defereggen – Antholz – Vals line and the Rieserferner tonalite to the north of the Staller Sattel recorded a multiphase structural and metamorphic history. Garnet-bearing assemblages in micaschists crystallized during development of foliations S_1 and S_2 by progressive deformation D_1-D_2. The strongly zoned garnets coexisted with micas and partly albitic plagioclase. This allowed to reconstruct an early prograde pre/syn-S_2 P-T evolution with a high-pressure stage (650°C/15 kbar) and a subsequent high-temperature amphibolite-facies stage (680°C/7 kbar) by cation-exchange and -net-transfer geothermobarometry. Truncation of S_2 by late-Variscan pegmatites as well as parallel linear-planar structures of D_1-D_2 in Upper-Ordovician granitoids and their host rocks, and similar garnet zonation trends in micaschists from adjacent basement parts with late-Variscan mica cooling ages, point to an early-Variscan age of this metamorphism. A presumably early-Alpine foliation S_{A1} with fine-grained muscovites overprinted the pegmatites and the earlier structures under greenschist-facies conditions of 450°C/3–4 kbar. Fine-grained recrystallization of paragonite and growth of post-S_2 and post-S_{A1} andalusite + staurolite and sillimanite + Kfeldspar + muscovite + quartz assemblages in some samples are related to a late-Alpine thermal metamorphism within the contact aureole around the 30 Ma old Rieserferner tonalite. Interpretation of the assemblages by petrogenetic grids yielded conditions of 620°C/2–3 kbar next to the pluton. Syncrystalline rotation of contact metamorphic porphyroblasts, monoclinal folding of S_2-S_{A1} domains, a foliation S_{A2} which deforms sigmoidal S_2-S_{A1} domains, and a shearband foliation S_{A3} are structures of a late-Alpine progressive shear zone deformation with phyllonitisation and mylonitisation along the northern margin of the Defereggen-Antholz-Vals line. In chlorite-muscovite phyllonites, fine-grained chlorite + muscovite + quartz in S_{A2}, chlorite + quartz in S_{A3}, and quartz fabrics signalize decreasing temperatures in course of this deformation. The corresponding kinematic criteria uniformly display a sinistral strike-slip movement in the shear zone.

1. Introduction

The late-Alpine Defereggen – Antholz – Vals line (DAV) subdivides the Austroalpine basement to the south of the Tauern Window into a northern block with Alpine metamorphism and ductile deformation, and a southern block which lacks pervasive Alpine ductile overprinting (HOFMANN et al., 1983; STÖCKHERT, 1985). In both blocks, the lithological units exhibit similar pre-Alpine histories; with Upper-Ordovician granitoid intrusions (BORSI et al., 1973; HAMMERSCHMIDT, 1981), followed by pervasive ductile shearing under high-pressure (SCHULZ, 1990; 1992; 1993) and subsequent amphibolite-facies conditions (STÖCKHERT, 1985; SCHULZ et al., 1993). In several parts of the basement, partial melting occurred during the high-temperature amphibolite-facies stage (HOKE, 1990). After separation from their crystalline residuum, the anatectic melts intruded (STÖCKHERT, 1987) into already foliated host rocks and formed aplitic and pegmatitic rocks with late-Variscan Rb-Sr whole-rock ages around 260 Ma (BORSI et al., 1980; HOKE, 1990). In the northern block, the pegmatites with coarse-grained magmatic muscovites suffered a deformation with formation of a penetrative foliation by fine-grained phengites. K-Ar data around 100 Ma from both mica generations suggest an early-Alpine minimum age of this overprinting (STÖCKHERT, 1984; 1987).

The regional distribution of late-Alpine Rb-Sr biotite cooling ages, ranging from 28 to 15 Ma from the southern to the northern part of the northern block and contrasting late-Variscan mica cooling ages in the southern block (BORSI et al., 1978), points to a considerable differential vertical movement component during sinistral strike-slip displacement along the Defereggen – Antholz – Vals line (BORSI et al., 1978; KLEINSCHRODT, 1987; SCHULZ, 1989). Displacement along this line survived the intrusion of the Rieserferner tonalite at 30 Ma (BORSI et al., 1979) and the formation of its metamorphic contact aureole (BECKE, 1892; BELLIENI & VISONA, 1981; PROCHASKA, 1981a; 1981b; MAGER, 1985; ZARSKE, 1985), but were completed previous to 20.5 Ma. This is obvious from apatite fission-track ages which are continuously younger from the southern to the northern parts of the basement (20.5 to 8.5 Ma) and which display a homogeneous post-Oligocene uplift of both blocks when combined with the Rb-Sr data (GRUNDMANN & MORTEANI, 1985).

Rocks of the Austroalpine basement crop out in the Staller Alm and Staller Sattel area in Eastern Tyrol, Austria, and can there be studied within well-exposed sites (Text-Fig. 1). This paper describes lithology and structures of the basement rocks and deals with microstructures, quartz fabrics, mineral chemistry and metamorphism of metapelites in a narrow slice of the northern block between the Defereggen – Antholz – Vals line (DAV) and the Rieserferner tonalite. In these rocks, microstructures, mineral parageneses and mineral compositions of successive stages of metamorphism and deformation remained preserved within low-strain zones or microlithons and allowed to reconstruct a multiphase evolution. The rocks with a complex pre-Alpine history were overprinted by presumably early-Alpine deformation and metamorphism, were affected by late-Alpine thermal metamorphism in the Rieserferner contact aureole and suffered late-Alpine shear-zone deformation along the DAV.

2. Lithology and Mesoscopic Structures in the Staller Sattel Area

Monotonous sequences with alternating biotite-plagioclase paragneisses, quartzitic gneisses and kyanite-staurolite-garnet-bearing micaschists are prevailing in the pre-Alpine metapsammopelitic unit (MPU) to the south of the Defereggen – Antholz – Vals line (DAV). Thin layers of calcsilicate-gneisses, graphitic gneisses, marble, amphi-

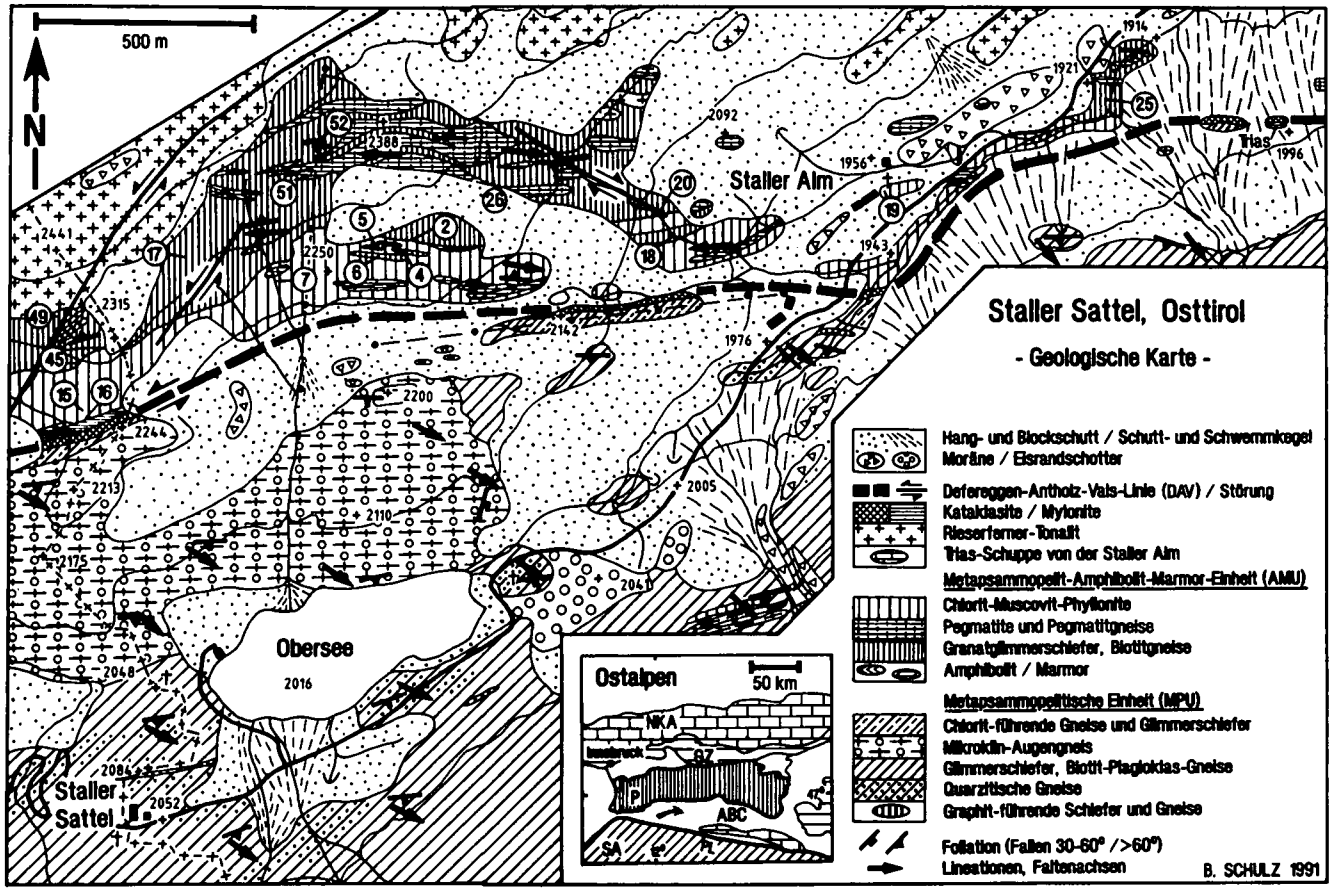

Text-Fig. 1.
Geological map of the Staller Sattel area, Eastern Tyrol, Austria.
Encircled numbers refer to sample descriptions in the text. Arrow in the small inset map points to the Staller Sattel region.
ABC = Austroalpine basement complex; GZ = Grauwacken-Zone; NKA = Northern Calcareous Alps; P = Penninic unit (Tauern Window); PL = Periadriatic Lineament; SA = Southern Alpine unit.

bolite and quartz-feldspar gneisses are rarely found. A dominant foliation S_2 (quartz layers are considered to represent an older S_1) is axial-planar to rare isoclinal and sheath-like F_2-folds.

In quartzitic gneisses and calcsilicate-gneisses a mineral lineation L_2 runs subparallel to the long axes of sheath folds and calcsilicate gneiss bodies (SCHULZ, 1988a, 1988b). F_2-folds and S_2 were refolded and overprinted by dominant open to tight F_3-folds and crenulations Cr_3 (Text-Fig. 3). The hinges of F_3-folds and the crenulation lineation Lcr_3 are mostly oriented parallel to L_2. F_3-folds with steeply SE-plunging hinges (Text-Fig. 2d) are minor structures of kilometre-scale "Schlingen" (SCHMIDEGG, 1936; BORSI et al., 1978; SCHULZ, 1988a), and can be observed along the Austrian-Italian border to the south of the Staller Sattel Pass (Text-Fig. 1).

Until now, no radiometric data is available from a leucocratic orthogneiss with microcline augen to the north of the Obersee (Text-Fig. 1). This orthogneiss can be assigned by lithological comparison only to the Upper-Ordovician granitoids in the basement as the Antholz (Anterselva) and Sand in Taufers (Campo Tures) orthogneisses. The main foliation of the ortho-augengneiss is composed of muscovite and biotite, the latter of which is mostly altered to chlorite. Obviously, the orientations of the main foliations and the lineations of the orthogneiss and its metapsammopelitic host rocks are parallel and display similar arrangements in the stereographic projections (Text-Fig. 2d, e). In combination with late-Variscan cooling ages in the southern block (BORSI et al., 1978), these parallel

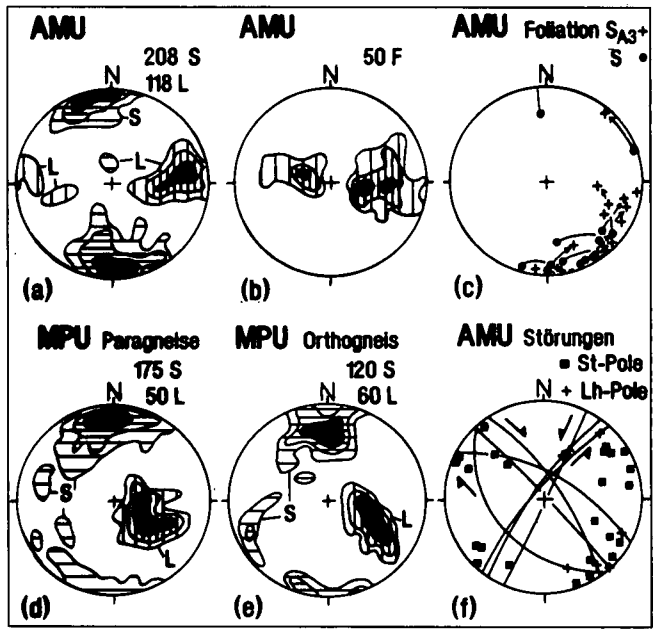

Text-Fig. 2.
Tectonic diagrams from the Staller Sattel area.
Projection of poles in > 1 %, >3 %, >5 % isolines into the lower hemisphere.
AMU = metapsammopelite-amphibolite-marble unit to the north of the Defereggen – Antholz – Vals line (DAV); MPU = metapsammopelitic unit to the south of the DAV; F = fold axes; L = lineations; Lh = slickenside striae; S = foliation; Sh = slickenside planes.

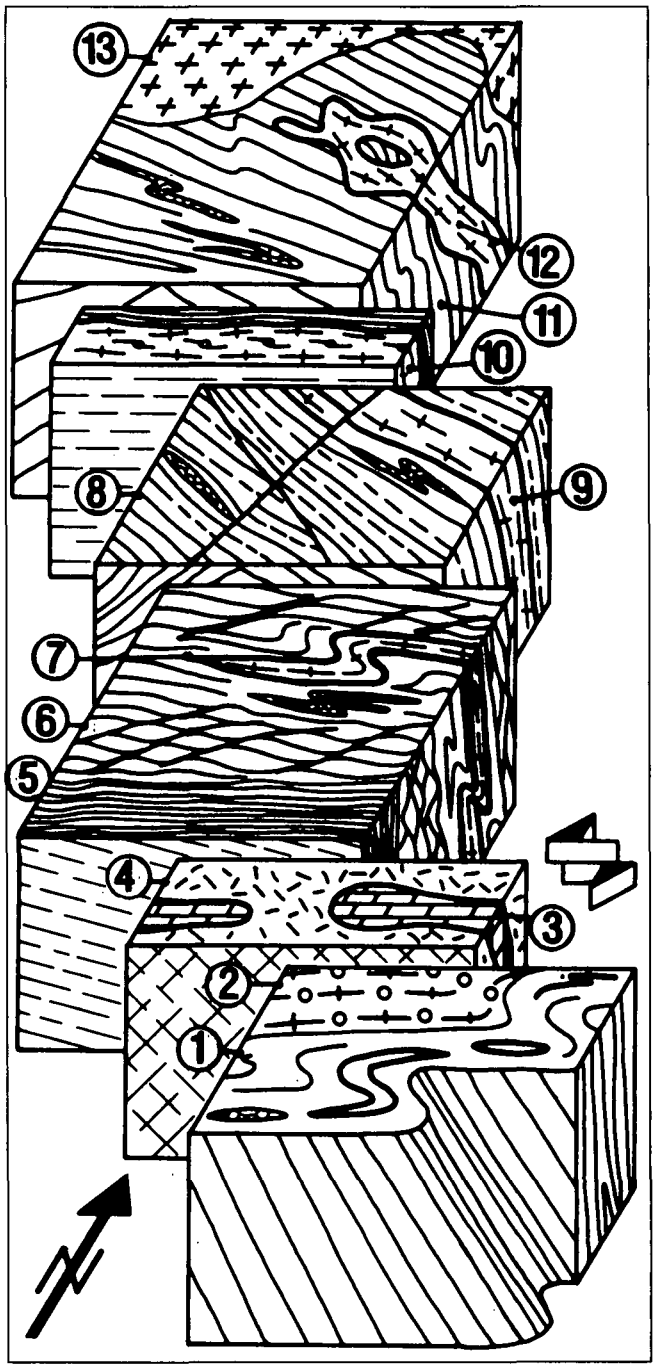

Text-Fig. 3.
Mesoscopic structures in basement rocks of the Staller Sattel area in a schematic view.
1) Metasediments of the metapsammopelitic unit (MPU) to the south of the Defereggen – Antholz – Vals line (DAV) with isoclinal and sheath-like F_2-folds and steeply plunging F_3-folds.
2) Orthogneiss with microcline augen in the MPU.
3) Triassic carbonates in the southern cataclastic domain of the DAV.
4) Southern cataclastic domain of the DAV with chloritic micaschists and gneisses and various types of cataclasites.
5) Northern mylonitic domain of the DAV with fine-banded mylonites.
6) Chlorite-muscovite-phyllonites with a shearband foliation S_{A3}.
7) Pegmatite (probably late-Variscan) with a foliation S_{A1} which forms a monoclinal fold.
8) Micaschists and biotite gneisses of the metapsammopelite-amphibolite-marble unit (AMU) to the north of the DAV with foliations S_2 (lines) and S_{A1} (broken lines), S_1 quartz layers and F_2-folds. A system of conjugated strike-slip faults cuts across the basement rocks.
9) Foliated (S_{A1}) late-Variscan pegmatite.
10) discrete shear zone with a mylonitized pegmatite.
11) Biotite gneisses and micaschists with the pre-Alpine main foliation S_2.
12) Undeformed late-Variscan pegmatite which cuts across older structures.
13) Late-Alpine Rieserferner tonalite.

fabrics signalize a common post-Upper-Ordovician and pre-late-Variscan polyphase deformation (D_1–D_2 and D_3) of both rock types (STÖCKHERT, 1985; SCHULZ, 1988a; 1990).

Chloritic quartzitic gneisses and chloritic micaschists, various types of cataclasites and an intercalated slice of Triassic carbonates (SENARCLENS-GRANCY, 1932; 1964; 1972) of the southern brittle deformation domain of the Defereggen – Antholz – Vals line (DAV) mark the border of the southern block (SCHULZ, 1989). Within the adjacent northern ductile deformation domain of the DAV, a transition from ultra-mylonites, mylonites and blasto-mylonites to chlorite-muscovite phyllonites of the northern block is observed (Text-Fig. 3).

Further to the north, a W–E-trending varied sequence with biotite gneisses, quartzitic gneisses, garnet micaschists, marbles, amphibolites, graphitic quartzites and numerous quartz-feldspar-pegmatites can be assigned to a metapsammopelite-amphibolite-marble unit (AMU) which contrasts the monotonous metapsammopelitic series of the MPU in the southern block of the basement. Next to the Rieserferner tonalite, a contact metamorphism of the metapsammopelites is evident from K-feldspar, sillimanite, andalusite and staurolite porphyroblasts, from grain coarsening of feldspar and quartz and from a darker colour due to the recrystallization of biotite. Structures and lithological banding of the metamorphic rocks are cut by the margin of the tonalite pluton. Radiometric data from the garnet-, tourmaline-, and muscovite-bearing quartz-feldspar-pegmatites is not yet available from the Staller Sattel region, however, a late-Variscan age of these rocks can be inferred from their lithological similarities to dated late-Variscan pegmatites elsewhere in the basement (BORSI et al., 1980; STÖCKHERT, 1984; 1987; HOKE, 1990). Unfoliated coarse-grained pegmatites which crosscut the foliated biotite-gneisses are observed at location 52 (Text-Figs. 1, 3). In contrast, at location 26 and other places, a planar penetrative foliation of the pegmatites by fine-grained muscovite-layers surrounding K-feldspar clasts and running parallel to the planar anisotropy of the host rocks, is obvious. Monoclinal folding of this foliation occurs at location 5. Furthermore, structural transitions from poorly foliated to strongly foliated pegmatites are abundant. At location 51 (Text-Figs. 1, 3) a fine-banded mylonitic pegmatite with broken and rotated Kfeldspar clasts and a flatly plunging lineation is found, forming a discrete mylonite zone in the northern block. These structural relationships allowed to distinguish between pre-Alpine foliations (S_1, S_2) which do not occur in the pegmatites but in their host rocks, and Alpine foliations (S_{A1}, S_{A2}, S_{A3}) which are found in both pegmatites and metapelites (Text-Figs. 3, 4).

Thin layers of pure quartz in biotite gneisses and garnet micaschists are interpreted to represent a foliation S_1. The steeply north and south dipping main foliation S_2 by coarse-grained micas is axial-planar to isoclinal F_2-folds of the quartz layers (Text-Fig. 3). Successive younger foliations S_{A1} by layers of fine-grained muscovite and S_{A2} by fine-grained chlorite and muscovite (see below) are parallel or subparallel to S_2 and overprint the rocks immediate

to the north of the DAV mylonites. There, S_2, S_{A1} and S_{A2} are folded into monoclinal tight folds with flatly to steeply W and E dipping hinge lines and with similarly oriented mineral elongation lineations on the foliation planes (Text-Fig. 2a, b). A shearband foliation S_{A3} with chlorite cuts the other planes at acute angles and with a sinistral offset (Text-Figs. 2c, 3). S_{A3} is dominant in the muscovite-chlorite phyllonites, dips steeply to the north and is associated with a flatly W or E plunging lineation (Text-Fig. 3).

Two systems of steeply dipping NW–SE- and NE–SW-striking strike-slip faults crosscut the earlier structures (Text-Figs. 1, 2f, 3). A subhorizontal dextral offset of 20 m has been observed along a NW-trending fault; the NE-striking faults display a sinistral displacement. Both fault systems appear to be conjugated, cut across the mylonites of the DAV and can be related to a subhorizontally N–S-directed compression (ANGELIER & MECHLER, 1977).

3. Microstructures to the North of the DAV

3.1. Microstructures in Metapelites

The microstructures of metapelites to the north of the DAV (67 samples) were studied in XZ-sections parallel to and in YZ-sections perpendicular to the lineation X. It was possible to distinguish between five successive generations of foliations S_1, S_2, S_{A1}, S_{A2} and S_{A3} (Text-Fig. 4). Crenulated S_1 in garnet micaschists is preserved within microlithons or enclosed as S_1i in garnet porphyroblasts (Text-Fig. 4a). S_2 appears as an axial-planar foliation to the microfolds and surrounds the microlithons. Coarse-grained micas underline both foliations. A foliation S_{A1} by planar mm-thick domains composed of fine-grained muscovites is oriented parallel to S_2 (Text-Fig. 4b). In chlorite-muscovite phyllonites, a fine-grained foliated matrix S_{A2} by muscovite, chlorite and quartz is pervasive. Sigmoidal domains of preserved S_2 and S_{A1} are surrounded by S_{A2} (Text-Fig. 4c). The shearband foliation S_{A3} cuts S_{A2} at acute angles (30°) with a sinistral sense of offset (Text-Fig. 4d).

Minerals inside microlithons are interpreted to have grown earlier than minerals composing the surrounding foliations. Correspondingly, all minerals which enclose traces of a foliation crystallized during or after the generation of that foliation (SPRY, 1969; VERNON, 1978; BELL et al., 1986). During later stages of metamorphism, porphyroblasts can be replaced or accompanied by other minerals in pressure shadows. This way it is possible to ascertain the relative time of crystallization of each mineral by using its microstructural position with reference to the successive foliations.

In garnet-micaschists, large first generation garnets (Grt_1) overgrew the crenulated S_1 underlined by biotite 1 and muscovite 1 (Bt_1, Ms_1), plagioclase 1 (Pl_1), quartz and opaques or enclose a planar S_1i (Text-Fig. 5c, f). S_2 composed of biotite 2 and muscovite 2 (Bt_2, Ms_2) surrounds the microlithons with the folded S_1, the garnet 1, a second generation of smaller garnets (Grt 2) without inclusions, plagioclase 2 (Pl_2) and quartz (Text-Fig. 5a–e). A first generation of staurolite (St_1) is rarely found elongated in S_2. From the porphyroblast-S_1i and matrix-S_2 relationships it can be suggested that S_1 and S_2 have been formed successively in course of a progressive deformation D_1-D_2. During the development of foliation S_{A1} or later, garnets within the S_{A1} as well as in the S_2 domains were broken and their fragments drifted along the tension cracks (Text-Fig. 6b).

Mineral parageneses of a thermal contact metamorphism near to the Rieserferner intrusion are restricted to the basement rocks to the north of the DAV. A subdivision of the contact metamorphic aureole around the tonalite into distinct sillimanite-, andalusite- and staurolite-zones (MAGER, 1985) and additional garnet and biotite zones (PROCHASKA, 1981a; CESARE, 1991) as in the flat-lying metapsammopelites on the top of the pluton, has not been carried out along the steeply dipping flank of the intrusion at the Staller Sattel.

Within 100 m distance to the pluton, biotite gneisses bear both fibrolitic and euhedral sillimanite, andalusite, Kfeldspar and muscovite. In sample 49, the foliation S_{A1}–S_{A2} by biotite and fibrolitic sillimanite surrounds sigmoidal microlithons with small andalusite grains and euhedral sillimanite which are mantled by muscovite (Text-Fig. 6i, k). This possibly indicates a conversion of euhedral andalusite and sillimanite to fibrolitic sillimanite by ionic reaction cycles (CARMICHAEL, 1969). The long axes of the large muscovite, aluminosilicates and of K-feldspar are oriented oblique in reference to the surrounding foliation and suggest a slight syn- to postcrystalline porphyroblast rotation by sinistral shearing. Garnet micaschists bearing andalusite (And) and second generation staurolite (St_2) occur at larger distances (>100 m) away from the Rieserferner intrusion.

The crystallization of andalusite and staurolite 2 postdates S_2, the development of S_{A1} with the fine-grained muscovites and the brittle deformation and fragmentation of the garnets. This is evident from a crystallization of the porphyroblasts within S_{A1} domains (Text-Fig. 6c), inclusion trails lining up with the external S_2 and S_{A1} foliations (Text-Fig. 6c, e–h) and from enclosed broken garnets in andalusite and staurolite 2 (Text-Fig. 6d, f, g). Some of the andalusites and staurolites display structures of syn- and postcrystalline rotation. Their straight or slightly curved inclusion trails Si are oriented oblique to S_2 or S_{A1} but are lining up with the external foliation (Text-Fig. 6e–h).

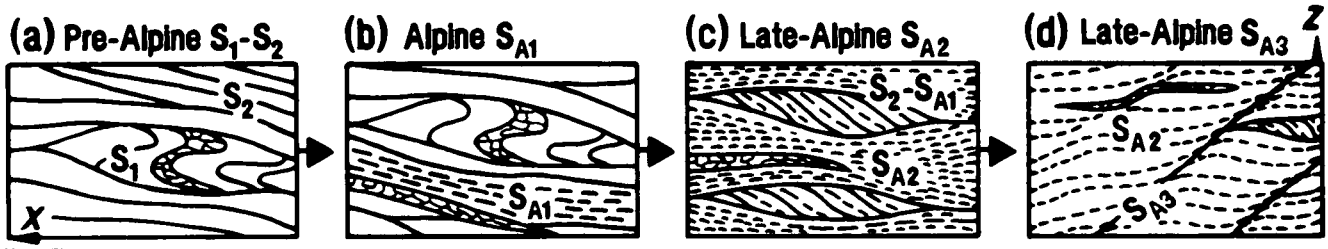

Text-Fig. 4.
Development of the successive foliations S_1, S_2, S_{A1}, S_{A2}, S_{A3} and the microstructural domains in micaschists (a, b) and chlorite-muscovite phyllonites (c, d) to the north of the Defereggen – Antholz – Vals line in a schematic view.

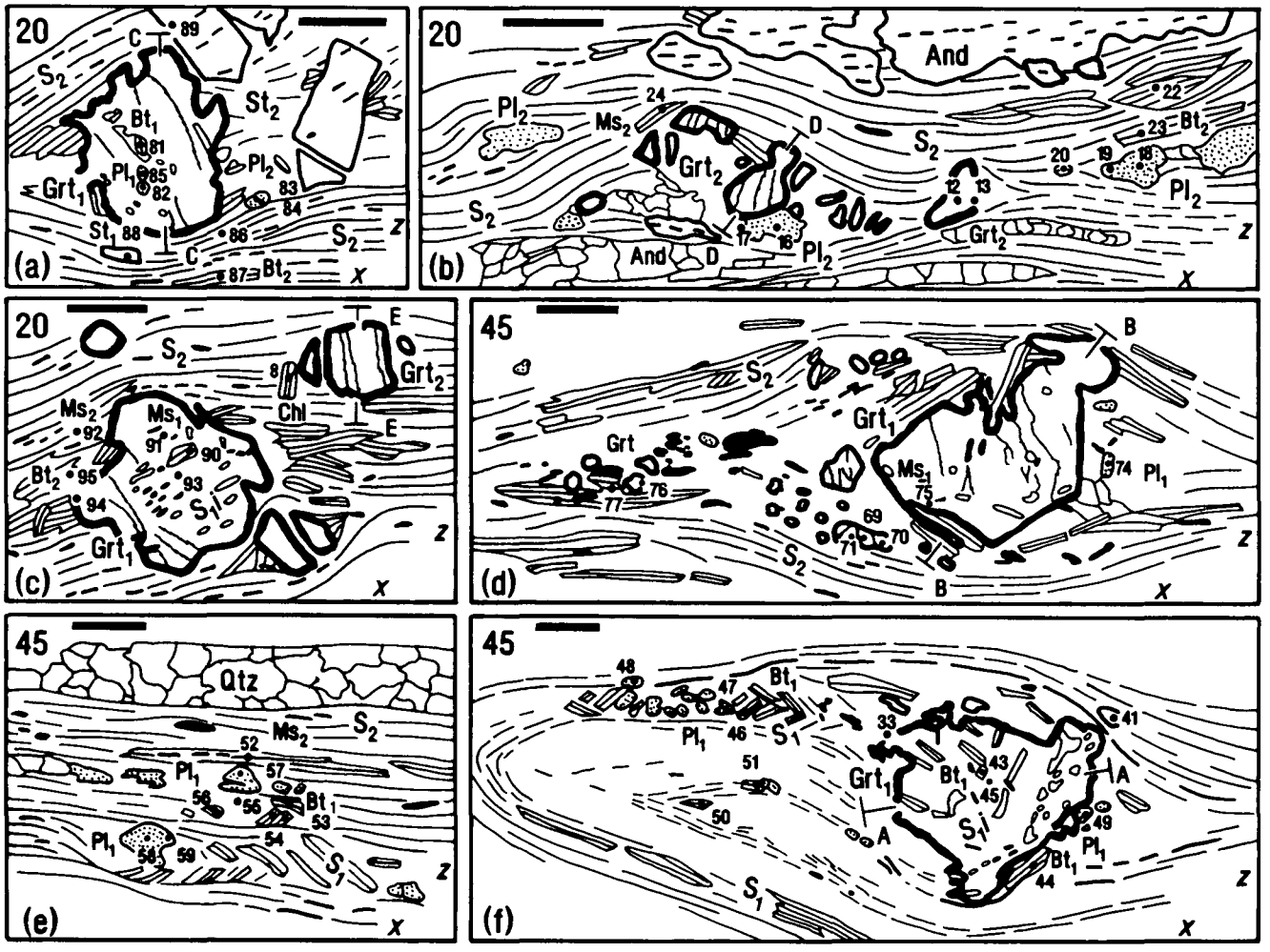

Text-Fig. 5.
Microstructures of pre-Alpine evolution in micaschists to the north of the Defereggen – Antholz – Vals line.
Large numbers refer to sample locations in Text-Fig. 1, small numbers indicate microprobe analyses in Text-Fig. 8 and Table 1, for zonation profiles of garnets see Text-Fig. 8a–e. All sections are parallel to the lineation (X), W is to the left. Scale bar = 1 mm.
a) First generation garnet (Grt) enclosing biotite (Bt) and plagioclase (Pl). Presumably pre-Alpine Staurolite 1 (St) appears in foliation S_2, staurolite 2 of late-Alpine contact metamorphism is post-S_2.
b) Second generation garnet (broken) in a microlithon with plagioclase. Andalusite of contact metamorphism is post-S_2.
c) Large garnet 1 with S_1 i in microlithon and garnet 2 within foliation S_2.
d) Microlithon with large garnet 1, surrounded by S_2.
e) Foliation S_2 surrounds small microlithons with crenulated S_1 by micas and plagioclase.
f) Microlithon with large garnet 1 which overgrew a folded foliation S_1 by micas, quartz and opaques.

Several microstructural domains can be distinguished in the chlorite-muscovite phyllonites to the north of the DAV line. Relics of the foliations S_2 and S_{A1} – coarse-grained S_2 micas are partially to completely fragmented into small sheets – are preserved in sigmoidal domains within a fine-grained foliated matrix S_{A2} by muscovite, chlorite and quartz (Text-Fig. 6l, m). Similarly, optically zoned plagioclase and garnet were protected in microlithons from shearing along S_{A2}-planes (Text-Fig. 6m). The fine-grained S_{A2}-domains are high-strain zones which cut the low-strain S_2-S_{A1}-domains at acute angles with a sinistral sense of movement (Text-Fig. 6l). Towards the south and towards the mylonitic part of the DAV, a modal increase of the S_{A2}-domains is observed in the rocks. S_{A2}-domains in chlorite-muscovite phyllonites as well as the foliations S_2 and S_{A1} of the micaschists are cut by a shear-band foliation S_{A3} with a sinistral sense of offset (Text-Fig. 6n). In the phyllonites, the lateral distances between S_{A3} domains are less than 1 cm, larger and more irregular spacing of S_{A3} is found in the micaschists further to the north.

To sum up, relics of older foliations and of earlier mineral generations remained preserved within low-strain domains ("microlithons") which are surrounded by high-strain domains or foliations of younger deformations. The relative temporal range of the foliations S_1, S_2, S_{A1}, S_{A2} and S_{A3} is obvious from the offset relationships (Text-Fig. 4). Furthermore, the microstructures described above allow to recognize a temporal range of mineral crystallization and mineral assemblages by porphyroblast – matrix and inclusion – foliation relationships. Accordingly, in samples 45 and 20, the crystallization of an assemblage with garnet + biotite + muscovite + plagioclase + quartz (Bt_1, Bt_2, Ms_1, Ms_2, Pl_1, Pl_2, Grt_1, Grt_2) is associated with the development of foliations S_1 and S_2. Probably, in sample 20 this assemblage is completed by staurolite 1 which appears elongated in S_2. Grain-size reduction of muscovite and brittle behaviour of garnet during generation of S_{A1} then signalize relatively low temperatures. Decussate recrystallization of muscovites in S_{A1} and crystallization of andalusite + staurolite 2 and of andalusite + sillimanite + Kfeldspar + muscovite postdate the S_2 and S_{A1} folia-

tions and can be related to a thermal metamorphism in the Rieserferner contact aureole. Syn- to postcrystalline rotation of the contact metamorphic porphyroblasts by sinistral movement, sinistral offset of older S_2-S_{A1} domains by S_{A2} (muscovite + chlorite + quartz) and sinistral offset along S_{A3} shearbands (chlorite + quartz) are assigned to progressive deformation along the Defereggen – Antholz – Vals line (DAV). This deformation evolved during decreasing temperatures, overprinted a part of the metapsammopelites of the basement and led to the development of chlorite-muscovite phyllonites at the northern margin of the line.

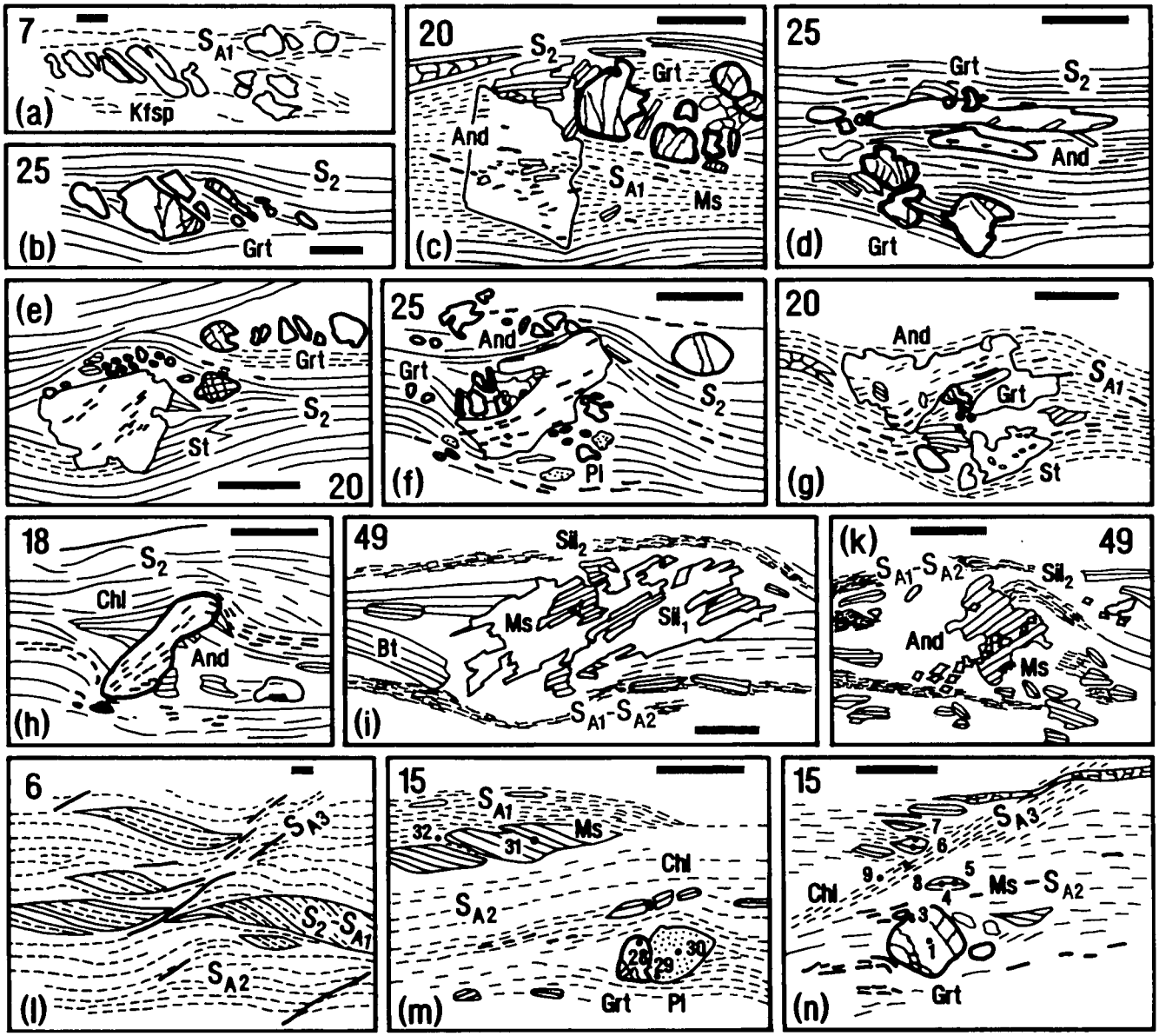

Text-Fig. 6.
Microstructures of Alpine evolution in micaschists and chlorite-muscovite phyllonites to the north of the DAV.
Large numbers refer to sample locations in Text-Fig. 1, small numbers indicate microprobe analyses in Text-Fig. 8 and Table 1. All sections are parallel to the lineation (X), W is to the left.
Scale bar = 1 mm.

a) Broken Kfeldspar (Kfsp) with tension cracks oblique to the surrounding foliation S_{A1} in a pegmatite.
b) Broken garnet with tension cracks oblique to the surrounding foliation S_2 in a micaschist.
c) Foliation S_{A1} by fine-grained muscovite (broken lines) in a micaschist was overgrown by andalusite of contact metamorphism.
d) Andalusite of late-Alpine contact metamorphism encloses broken garnet.
e) Staurolite of contact metamorphism encloses S_2 and S_{A1} and displays slight syncrystalline rotation with the internal foliation Si lining up with the external foliation Se.
f) Syncrystalline-rotated contact metamorphic andalusite encloses broken garnet.
g) The slightly curved internal foliation in the rim of an andalusite lines up with the external S_{A1} and indicates a syncrystalline rotation of the porphyroblast.
h) Syncrystalline-rotated andalusite of contact metamorphism with Si oblique and lining up with Se.
i,k) Euhedral sillimanite 1 (Sil1) and andalusite (And) grains of contact metamorphism are mantled by muscovite. Sillimanite and muscovite are oriented oblique in reference to a surrounding foliation by fibrolitic sillimanite 2.
l) Domains of foliation S_{A2} by fine-grained chlorite-muscovite-quartz (broken lines) surround sigmoidal domains of S_2 and S_{A1} by large and small muscovite in a phyllonitic micaschist.
m) S_{A2} in a chlorite-muscovite phyllonite surrounds relic garnet and plagioclase and domains with large muscovite and S_{A1}.
n) A shearband foliation S_{A3} with fine-grained chlorite and quartz deforms older foliation and quartz layers.

3.2. Quartz Fabrics

Quartz fabrics and quartz-c axes orientations were studied in XZ-sections (parallel to the lineation, perpendicular to the foliation) from several samples with mm-thick planar or tightly folded (sample 2) monomineralic quartz layers. The layers are concordantly interlayered in the foliated matrix of metapelites and pegmatites (samples 5-1, 5-2, 7). Two principally different distributions of quartz-c axes in lower hemisphere projections are observed (Text-Fig. 7) in the samples, in one sample (5) both types occur. According to the models of LISTER & HOBBS (1980), the quartz-c fabrics in samples 4, 5-1, 7, 18-1, 20, 25 (Text-Fig. 7a–e, h) indicate coaxial deformation with axial extension in the X (= lineation) direction. Quartz grains in these samples are 0.2–0.6 mm in diameter and display straight or slightly curved stable grain boundaries. Within the grains, indications of plastic deformation or subgrain-formation are lacking. At triple junctions, grain boundaries are often drawn into equilibrium angles of 120° and indicate static grain growth. This allowed to conclude that these fabrics were formed at temperatures considerably exceeding 300°C (VOLL, 1976).

Inclined single girdle distributions of quartz-c axes orientations in samples 15, 16, 17, 19, 52, monoclinic distributions of c-axes maxima in samples 5-2, 6, 18-2, and cross girdles with asymmetric maxima as in the long limb of a monoclinal fold in sample 2 (Text-Fig. 7f, g, i–p), signalize a non-coaxial deformation history when interpreted using the models of LISTER & HOBBS (1980). Maxima of c-axes poles are situated near the rims and intermediate parts of the projection nets and point to a dominant activity of basal and rhombohedral glide systems during deformation (BOUCHEZ & PECHER, 1981). The oblique orientation of the monoclinic c-axes fabrics indicates a sinistral sense of shear (BEHRMANN & PLATT, 1982) which is in accordance with shear sense indications by oblique tension cracks of porphyroclasts (Text-Fig. 6a, b), porphyroblast rotations (Text-Fig. 6 e–k) and the offset by S_{A2} and S_{A3} domains (Text-Fig. 6 l–n). In samples with monoclinic quartz-c fabrics but lacking S_{A2} domains (2, 17, 52), coarse quartz grains (0.3–1.0 mm) occur. The grain boundaries are strongly curved and sutured and display preferred orientation (Text-Fig. 7g, k, l). In samples with high mode of S_{A2} domains (5-2, 15, 16, 19), the quartz grains with preferentially oriented and strongly sutured grain boundaries are smaller than 0.2 mm (Text-Fig. 7i, n–p). Recrystallization by formation of new grains (diameter around 0.05 mm) along grain boundaries is frequent. These microstructures are characteristic of dynamic recrystallization at temperatures moderately above 300°C (VOLL, 1976). A strong plastic deformation of the grains is observed when monomineralic layers of fine-grained (<0.2 mm) quartz are deformed in S_{A3} domains. Aspect ratios up to 1 : 10 with elongation of the grains parallel to S_{A3} are found. These quartz fabrics indicate temperatures around or slightly above 300°C during development of S_{A3} (VOLL, 1968; 1976).

To sum up the observations from the quartz layers, a presumably earlier phase of coaxial deformation can be related to temperatures considerably exceeding 300°C. A later second phase of non-coaxial deformation with sinistral sense of shear overprinted the earlier fabrics and was accompanied by progressive grain-size reduction and dynamic recrystallization of quartz. In course of this deformation, temperatures moderately exceeded 300°C, but fell below the thermal conditions of the precedent deformational stage. A final step of non-coaxial deformation at temperatures around 300°C proceeded during the formation of S_{A3}.

4. Mineral Chemistry and Geothermobarometry

4.1. Mineral Chemistry in Metapelites

Microprobe analyses (130 points, for representative analyses see Table 1) were taken from garnet micaschists (samples 20 and 45), and from a chlorite-muscovite phyllonite (sample 15). Garnets display continuous growth zonations with variable almandine (Alm), spessartine (Sps), grossular (Grs) and pyrope (Prp) contents which allowed to evaluate a relative temporal evolution of the mineral chemistry by core-rim profiles. In the large first generation porphyroblasts of sample 45, spessartine contents evolve from 10 % in the cores to 5 % in the rims. Pyrope contents decrease (from 10 % to 4 %), then increase up to 10 % while the grossular contents first increase (7 to 25 %), then decrease (from 25 % to 10 %) and finally re-increase up to 20 % (Text-Fig. 8a). The early stage of decreasing pyrope contents is lacking in other porphyroblasts (Text-Fig. 8b). Plagioclases in the microlithons surrounded by S_2 display two trends of slight zonations, a probably older group with 24 % to 31 % anorthite (An) from cores to rims, and another group with An 31 % in the cores to An 27 % in the rims. Biotite 1 enclosed by garnet has lower XMg (0.36) compared to biotite 2 in the foliation S_2 (XMg 0.45–0.48). AlVI contents (from 0.71 to 0.84, always per formula unit, p.f.u.) and Ti (0.18–0.21) vary similarly in both generations of biotite. Muscovite 1 enclosed by garnet and muscovite 2 in S_2 have similar compositions with Na = 0.16–0.19, Si = 6.12–6.20, Fe = 0.14–0.17 and Mg = 0.14–0.17 (Text-Fig. 8n).

Cores of large first generation garnets in sample 20 display high spessartine contents (7–6 %) and decreasing grossular contents (9 to 4 %) at constant pyrope contents of 10 % (Text-Fig. 8c). A second generation porphyroblast inside a microlithon (Text-Fig. 5b) has low pyrope (10 %), low grossular (2 %) and high spessartine (8 %) contents in the core and high grossular (10 %) at low spessartine (2 %) contents in the rim (Text-Fig. 8d). Decrease of grossular (8–2 %) and spessartine (2–1 %) and significant increase of pyrope (11–15 %) from core to rim are observed from a second generation garnet in the foliation S_2 (Text-Fig. 8 e). The rims of the first generation porphyroblasts (Text-Fig. 8c) have similar compositions as second generation garnet rims with low Ca and high Mg contents (Text-Fig. 8 e, g), and rims of both porphyroblast generations seem to have grown simultaneously. Albitic plagioclase (An 4 %) is enclosed by garnet 1 (Text-Fig. 5a). A slightly zoned albitic plagioclase with An 6–7 % occurs in a microlithon with broken garnets 2 (Text-Fig. 5b). Other plagioclases in the microlithons and in S_2 are albitic as well. The Ca-poor and Mg-rich rim of a garnet 1 is associated with a slightly zoned oligoclase (An 14–16 %, Text-Fig. 5 a). Staurolite 1 in S_2 has lower XMg (0.15) than the core of a post-S_2 second generation porphyroblast (XMg 0.19). Biotites 1 inside garnet and biotite 2 in S_2 have similar XMg (0.45 -0.48), AlVI (0.85–0.91) and Ti (0.15–0.17) contents. Compositions of muscovite 1 and 2 are similar as well and Si (6.15–6.24), Na (0.33–0.44), Fe (0.09–0.16) and Mg (0.09–0.26) vary without relationship to the micro-

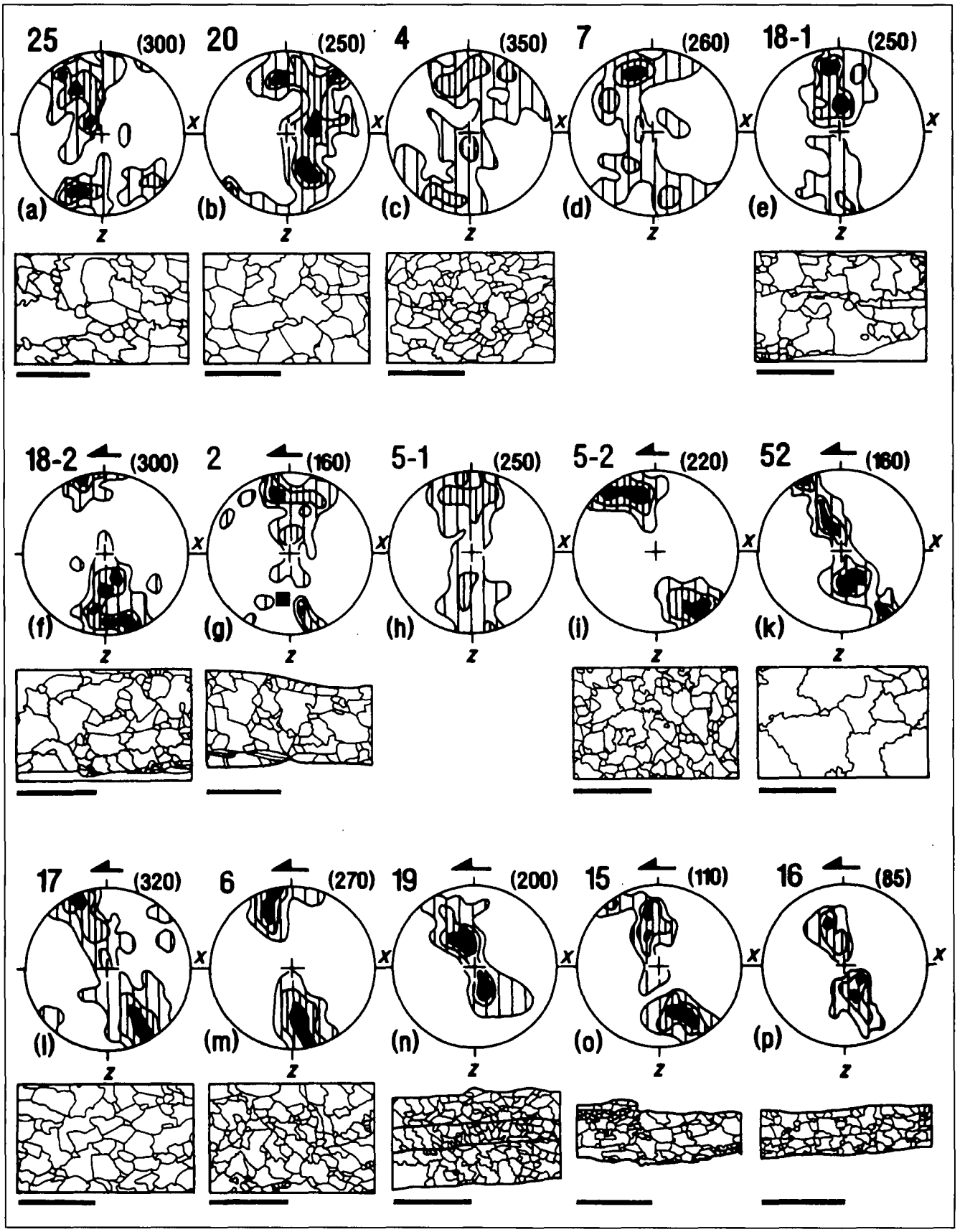

Text-Fig. 7.
Quartz fabrics in metapelites and foliated pegmatites (d, h, i) to the north of the DAV.
Large numbers refer to sample locations in Text-Fig. 1. Quartz-c axes poles (numbers in brackets) in >1 %, >3 % and >5 % isolines are projected into the lower hemisphere of a SCHMIDT net, the diagrams are oriented uniformly with the X axes (= lineation) in W–E direction (W is to the left).
Arrows indicate shear sense of hangingwall.
Scale bar = 1 mm.

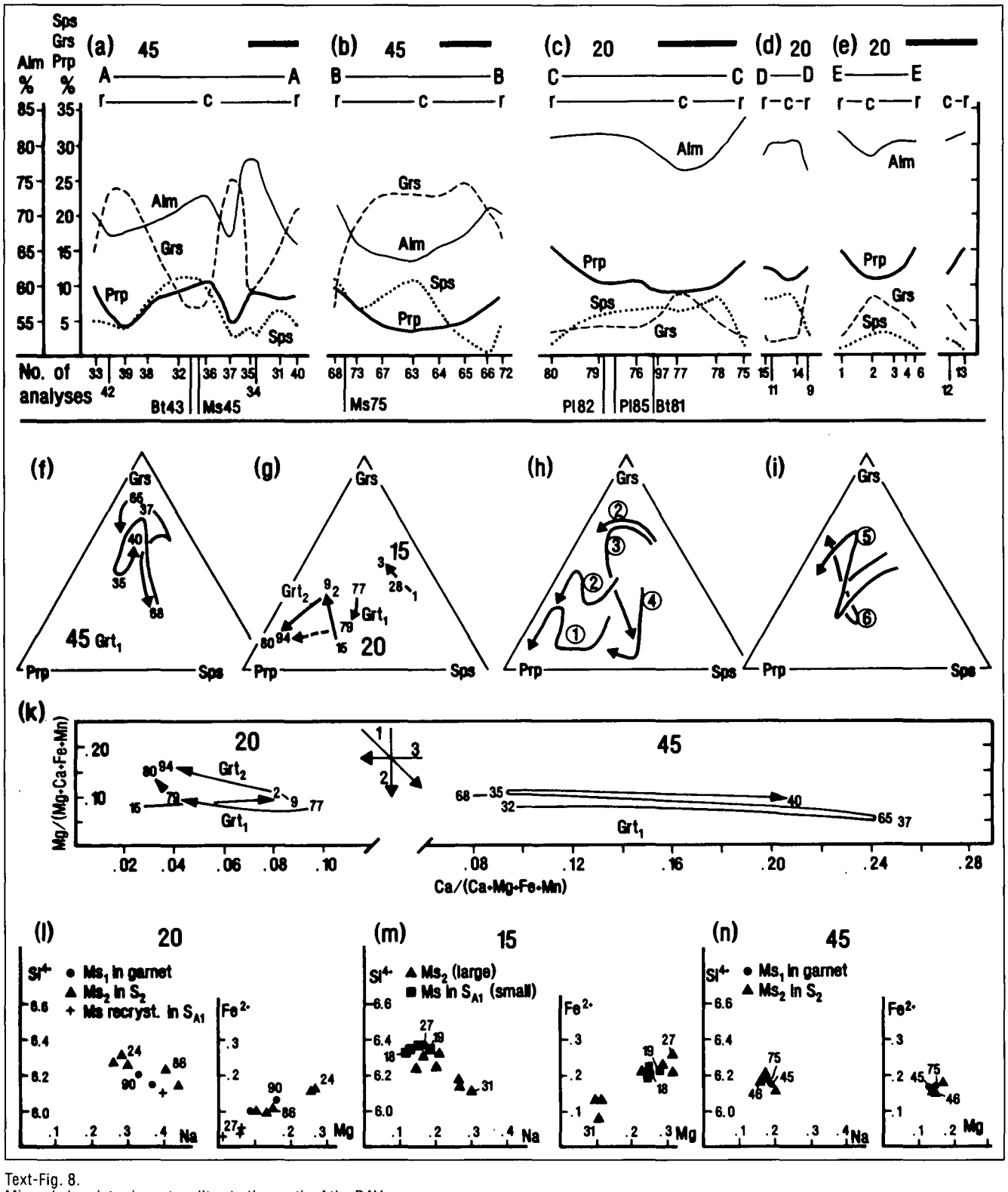

Text-Fig. 8.
Mineral chemistry in metapelites to the north of the DAV.
Large numbers refer to sample locations (Text-Fig. 1), small numbers indicate analyses in Text-Figs. 5, 6, 9 and in Table 1.

a–e) Garnet zonation profiles (c = core, r = rim) in almandine (Alm), grossular (Grs), pyrope (Prp) and spessartine (Sps) mole-%. Scale bar = 1 mm.

f,g) Chemical evolution of garnets in samples 45, 20 and 15 in grossular-pyrope-spessartine (Grs-Prp-Sps) coordinates. Arrows indicate temporal direction (from cores to rims) of the evolution.

h,i) Chemical evolution of garnets in micaschists from adjacent parts of the Austroalpine basement to the south of the Tauern Window, for comparison.
1 = Prijakt area, Schobergruppe, near to eclogitic amphibolites, lower part of the MPU (SCHULZ, 1991; 1993); 2 = southern Deferegger Alps to the south of St. Jakob, lower part of the MPU (SCHULZ, 1990); 3, 4 = southern Deferegger Alps to the south of St. Veit, upper part of the AMU (SCHULZ, unpublished data); 5, 6 = southern Deferegger Alps, upper parts of the MPU (SCHULZ, 1990, 1992, and unpublished data).

k) Evolution of garnet compositions in the *X*Mg versus *X*Ca diagram of MARTIGNOLE & NANTEL (1982). Chemical trends in the diagram refer to tectonic history: isobaric cooling (1), cooling/unloading (2) and isothermic unloading (3).

l–n) Mineral chemistry of muscovites in Si versus Na and Fe versus Mg diagrams.

structural position of the phyllosilicates (Text-Fig. 8l). However, some fine-grained recrystallized muscovites in a S_{A1} -domain display different paragonitic composition with high Na (0.90–1.26), very low Si (6.0–6.15), low Fe (0.04). low Mg (0.01–0.03) and reduced K (0.27–0.66 contents (Text-Fig. 8l) which suggest high temperatures during the recrystallization (see below).

Relic garnets in the chlorite-muscovite phyllonite of sample 15 are rich in spessartine (16–9 %) and grossular (12–15 %), and poor in pyrope (4 %) contents (Text-Fig. 8 g). Plagioclase is zoned with decreasing anorthite contents from cores to rims (8–2 %). Biotite was completely replaced by chlorite and titanite. The coarse-grained muscovites in S_2 display considerable variations of Na (0.17–0.30), Si (6.11–6.38), Fe (0.11–0.23) and Mg (0.08–0.29) contents. Sheared and recrystallized rims of the large muscovites and fine-grained muscovites in S_2, S_{A1} and S_{A2} domains are Si-, Fe-, Mg-rich and Na-poor (Text-Fig. 8m).

4.2. P-T Conditions of Metamorphism

The pre/syn-S_2 assemblage garnet + biotite + muscovite + plagioclase + quartz in samples 45 and 20 appears in a divariant field which is bounded by a garnet-forming reaction at low temperatures and a staurolite-producing reaction at high temperatures. Increasing *X*Mg of the zoned garnets are characteristic of a metamorphism prograde in temperature (MARTIGNOLE & NANTEL, 1982). According to the decreasing *X*Ca and the increasing *X*Mg in rims of second generation garnet, staurolite 1 in sample 20 probably was produced during decreasing pressure and increasing temperature by continuous reactions: garnet + chlorite + muscovite = staurolite + biotite + H_2O, or garnet + biotite + Al_2SiO_5 + H_2O = staurolite + muscovite + quartz (SPEAR & CHENEY, 1989). Changes in garnet composition can be explained by continuous reactions among garnet, biotite, muscovite and plagioclase inside the divariant field, depending on P and T (THOMPSON, 1976; TRZCIENSKI, 1977; TRACY, 1982). It is possible to use the garnet zonation trend within low-variance assemblages to derive $\Delta T/\Delta P$ trends by the Gibbs method (SPEAR & SELVERSTONE, 1983; SPEAR et al., 1984; HAUGERUD & ZEN, 1991). Each step of garnet chemical evolution represents a finite temporal and spatial domain of equilibration with the other minerals of the assemblage. Thus, when coexistent minerals are preserved as inclusions or within the microstructural domain of interest ("local equilibrium"), and when their chemical compositions are known, P and T can be evaluated by "conventional" thermobarometry (PERCHUK et al., 1985; TRIBOULET & AUDREN, 1985; ST-ONGE, 1987; HAUGERUD & ZEN, 1991).

However, each generation of mica seems to have been homogenized after a finite time interval of deformation (TRIBOULET & AUDREN, 1985). Despite a strong increase of *X*Mg in the garnets of sample 20 and in the outer parts of garnets in sample 45, corresponding biotites show only slight changes in Mg contents. In sample 45, garnets show significant Ca variations whereas the An-contents of the plagioclases only slightly vary between 24 and 31 %. High Ca contents in intermediate zones of the garnets are balanced by An-poorer cores of older plagioclase, and low Ca contents in garnets seem to correspond to the An-richer rims of the older plagioclase or to the cores of the younger plagioclase. The Ca-rich outer rim of one garnet then appears to coexist with the slightly An-poorer rim of the younger plagioclase. Slow rates of post-entrapment volume diffusion in plagioclase will preserve original compositions of inclusions inside garnets (ST-ONGE, 1987). The only effective means of equilibration is for old plagioclase to dissolve partially or completely, and for new plagioclase of a different composition to grow (SPEAR et al., 1990). No textural signs of a retrograde albitisation of initially anorthite-richer plagioclase and of coexisting oligoclase and albite (ASHWORTH & EVIRGEN, 1985a) were found in sample 20. Thus, enclosed albitic plagioclase is considered to coexist with the Ca-rich core of the surrounding garnet 1 (Text-Fig. 5a). Furthermore, the Ca-poor core of garnet 2 in sample 20 appears to coexist with the An-richer core of the adjacent plagioclase (Text-Fig. 5b), whereas the Ca- and Mg-rich core of the garnet 2 in the foliation is in equilibrium with albitic cores of plagioclases in the same microstructural position (Text-Fig. 5b, c). The Mg-rich and Ca-poor outer rims of both garnet generations then are associated with the Ca-richest plagioclase observed in the sample, an oligoclase with An 16 % (Text-Fig. 5a). Following the microstructural and mineral chemical observations, the garnets in sample 20 are considered to have grown and coexisted with plagioclases An 4–16 % throughout the pre/syn-S_2 metamorphism.

Temperatures from the garnet-bearing assemblages in samples 45 and 20 were calculated by applying five garnet-biotite Fe-Mg exchange geothermometers (THOMPSON, 1976; HOLDAWAY & LEE, 1977; HODGES & SPEAR, 1982; GANGULY & SAXENA, 1984; PERCHUK & ARANOVITCH, 1984) to mineral pairs. Corresponding pressures were estimated by four garnet-plagioclase Ca-net-transfer geobarometers involving aluminosilicate (NEWTON & HASELTON, 1981; GANGULY & SAXENA, 1984; PERCHUK et al., 1985; KOZIOL & NEWTON, 1988). A former presence of kyanite in the assemblage is suggested from the metapelitic bulk compositions of the samples in AFM-projections, and has been assumed for the calculations. Presumably kyanite disappeared by further reaction involving muscovite (CARMICHAEL, 1969) or by a rapid transformation to andalusite (sample 20) in course of a late stage of metamorphism. However, as has been outlined by FROST & TRACY (1991), in each case calculations will give maximal possible pressure. Due to this questionable presence of kyanite in the assemblages throughout the garnet growth, the calibration of GHENT & STOUT (1981) which can be applied to assemblages lacking aluminosilicates has been used additionally. Minimal and maximal results from all applied geothermo-barometers define P-T fields encompassing the disagreements among all the calibrations.

By a first step of calculations, temperatures were calculated from garnet rims and adjacent biotite of S_2. For pressure estimations adjacent plagioclase or rims of plagioclase in adequate positions in microlithons were used. A garnet rim recorded conditions of 600°C/10 kbar in sample 45 and 680°C/7 kbar in sample 20 (Text-Fig. 9a, b). However, the garnet rims with maximal *X*Mg represent only the maximal temperature which has been recorded by the garnets individual chemical evolution, and temperatures of the actual thermal peak of metamorphism may have been higher (SPEAR, 1991). The analyzed garnets in sample 45 seem to have not recorded this thermal peak. Furthermore it is of interest for tectonic interpretations to evaluate the P-T evolution previous to the thermal peak and to construct P-T paths. For this second step of calculations, characteristic analyses out of the garnets Ca and Mg evolution trends (Text-Fig. 8f, g, k) were combined with analyses from micas and plagioclases which are enclosed

by the garnet, are situated within the same microlithon as the garnet or occupy an equivalent microstructural position, and represent a "local equilibrium" as is explained above (TRIBOULET & AUDREN, 1985; SCHULZ, 1990). This leads to P-T paths with marked decompressional and compressional events during increasing temperatures (Text-Fig. 9a, b, see captions to Table 1 for the mineral pairs used for the calculations). The garnets in samples 45 and 20 similarly recorded decompression/heating from 560°C/10 kbar to 590°C/5 kbar and a subsequent compression. Chemical evolution of garnets in sample 45 stopped in course of compression and the maximal pressures (650°C/15 kbar) and maximal temperatures (680°C/7 kbar) were estimated from a second generation garnet in sample 20 (Text-Fig. 9b). A calculation of P-T values from characteristical analyses out of the garnets chemical trend will provide a less faulty relative P-T evolution due to the easiest controllable and measurable garnet zonations and the potentially minor serious effects of diffusion upon interior parts of the profiles. The dependence of a calculated P-T path on garnets XCa and XMg evolution is intensified due to the slight compositional variations of coexisting micas and the oppositely directed Ca zonation trends in the plagioclase. On the one hand, the P-T paths mainly follow the garnet Ca and Mg zonation trend and give a relative P-T evolution as from garnet zonation modelling. On the other hand, these paths are defined by actual P-T estimates, obtained from coexisting garnets, micas and plagioclases by "conventional" thermobarometry.

All geothermobarometric P-T estimates by cation-exchange and -net-transfer calibrations are afflicted with a quantitative minimum discord of 50°C/1 kbar. Uncertainties in the calculated P-T paths arise from microprobe analyses, thermodynamic data, combination of possibly inappropriate mineral pairs and the use of albitic plagioclase for pressure estimates from sample 20. Poorly understood activity/composition relationships in plagioclase An <20 % at low T (ASHWORTH & EVIRGEN, 1985a, b) and a possible strong positive deviation from ideality for plagioclase An<5–8 % (GHENT & STOUT, 1981) suggest that pressures calculated from garnet and albitic plagioclase may be doubtful and too high. Comparison of P-T estimates from eclogitic amphibolites and adjacent kyanite-staurolite-garnet micaschists with albitic plagioclase in the Schobergruppe (SCHULZ, 1991; 1992; 1993) indicate that pressures are overestimated by garnet-aluminosilicate-plagioclase barometers and underestimated by garnet-biotite-muscovite-plagioclase calibrations, and that mean values fit well with estimates from the metabasites

Table 1
Selected microprobe analyses of minerals from metapelites.
Numbers of oxygens: garnet 24; biotite and muscovite 22; chlorite 28; Staurolite 23.5. c = core, r = rim.
The following analyses were combined for geothermobarometry: Grt37 – Bt43 – Pl74 – Ms 45; Grt68 – Bt44 – Pl59 – Ms 75; Grt40 – Bt44 – Pl 61 – Ms 46; Grt79 – Bt81 – Pl82 – Ms90; Grt15 – Bt23 – Pl16 – Ms 90; Grt2 – Bt23 – Pl18; Grt94 – Bt95 – Pl83 – Ms 86; Grt80 – Bt95 – Pl83 – Ms86.
See Text-Figs. 5, 6 for microstructural positions of analyses.

Garnet

	sample 20										sample 45								sample 15	
	77c	79	80	75r	15r	9r	2c	6r	12c	13r	32c	37	35	40r	63c	65	68r	71	1c	3r
Si	6.04	6.01	5.98	5.96	5.88	5.93	5.93	5.88	5.96	5.92	5.90	5.93	5.95	5.94	5.99	5.93	5.95	5.92	5.92	5.95
Al	3.91	3.95	4.01	4.02	4.03	4.01	4.01	4.05	4.00	4.00	4.01	4.01	3.98	4.00	3.95	4.03	4.00	4.02	3.98	3.94
Fe	4.49	4.87	4.82	4.97	4.81	4.57	4.72	4.88	4.81	4.97	4.35	4.05	4.74	3.99	3.75	4.07	4.34	4.10	4.13	4.37
Mn	.35	.32	.08	.08	.47	.18	.19	.05	.11	.04	.67	.19	.23	.28	.67	.15	.67	.14	1.02	.93
Mg	.52	.58	.89	.79	.72	.71	.63	.91	.67	.90	.54	.29	.54	.51	.22	.29	.58	.65	.24	.28
Ca	.58	.23	.18	.16	.15	.60	.50	.24	.42	.20	.56	1.54	.56	1.27	1.40	1.51	.46	1.16	.74	.94
tot	15.89	15.96	15.96	15.98	16.06	16.00	15.98	16.01	15.97	16.03	16.03	16.01	16.00	15.99	15.98	15.98	16.00	15.99	16.03	16.41
Alm	75.56	80.95	80.56	82.81	78.10	75.42	77.96	80.05	80.02	81.20	70.91	66.80	77.86	65.95	62.01	67.47	71.52	67.83	67.29	71.24
Sps	5.91	5.33	1.40	1.35	7.68	3.01	3.18	.96	1.89	.73	11.01	3.26	3.93	4.67	11.19	2.59	11.12	2.32	16.66	8.91
Prp	8.80	9.78	14.93	13.16	11.78	11.71	10.55	14.95	11.17	14.73	8.92	4.79	8.95	8.47	3.73	4.93	9.70	10.73	3.99	4.59
Grs	8.78	3.79	3.01	2.57	2.24	9.63	8.05	3.89	6.58	3.25	9.02	24.94	9.19	20.75	22.93	24.80	7.62	18.80	11.92	15.13

	sample 20									sample 45						sample 15				
	Biotite				Muscovite				Chlorite	Biotite			Muscovite			Muscovite			Chlorite	
	81	23	95	29	90	86	24	27	8	43	44	55	45	46	75	18	19	27	31	33
Si	5.39	5.33	5.44	5.45	6.21	6.24	6.32	6.03	5.07	5.52	5.45	5.35	6.15	6.20	6.17	6.35	6.35	6.38	6.11	5.15
Ti	.15	.17	.17	.17	.04	.03	.05	.01	.02	.28	.21	.21	.03	.05	.05	.03	.03	.02	.05	.01
Al	3.52	3.56	3.41	3.40	5.55	5.55	5.32	6.04	5.80	3.27	3.27	3.42	5.63	5.58	5.63	5.21	5.16	5.10	5.65	5.65
Fe^{2+}	2.56	2.56	2.68	2.63	.13	.09	.16	.02	4.67	2.99	2.63	2.63	.16	.14	.17	.21	.23	.27	.11	5.25
Mg	2.15	2.11	2.11	2.14	.15	.13	.27	.01	4.40	1.69	2.15	2.13	.12	.14	.15	.24	.27	.31	.08	3.82
Na	.09	.03	.03	.07	.33	.40	.27	1.26	.01	.02	.05	.05	.19	.17	.16	.12	.19	.17	.30	.01
K	1.66	1.81	1.67	1.64	1.35	1.32	1.33	.27	.001	1.87	1.84	1.86	1.53	1.47	1.36	1.71	1.72	1.72	1.65	-
tot	15.52	15.57	15.51	15.50	13.76	13.76	13.72	13.64	20.06	15.64	15.60	15.65	13.81	13.75	13.69	13.87	13.95	13.97	13.95	19.89
XMg	.46	.46	.45	.45	-	-	-	-	.48	.36	.45	.45	-	-	-	-	-	-	-	.42

	Plagioclase																	Staurolite	
	sample 20									sample 45						sample 15			sample 20	
	82	85	16c	17r	18c	20	21	83c	84r	47	74	58c	59r	60c	61r	10c	11r		88	89
Si	2.94	2.97	2.93	2.93	2.96	2.92	2.95	2.82	2.84	2.65	2.72	2.67	2.65	2.66	2.69	2.90	2.95	Si	3.88	3.85
Al	1.04	1.02	1.08	1.07	1.05	1.06	1.03	1.17	1.15	1.34	1.27	1.31	1.33	1.32	1.29	1.10	1.05	Ti	.05	.04
Na	.95	.96	.85	.90	.87	.98	.99	.84	.83	.70	.75	.71	.69	.72	.74	.90	.91	Al	9.06	9.00
K	.003	.002	.003	.002	.003	.002	.003	.002	.003	.005	.008	.003	.005	.006	.003	.005	.003	Fe	1.26	1.35
Ca	.038	.015	.068	.061	.028	.054	.036	.158	.146	.32	.25	.31	.32	.31	.28	.082	.032	Mg	.21	.30
tot	4.97	4.96	5.04	4.96	4.94	5.01	5.00	4.99	4.96	5.01	4.99	5.00	4.99	5.01	5.00	4.98	4.94	Mn	.012	.013
An	3.91	1.51	7.36	6.31	3.11	5.17	3.53	15.80	14.83	31.46	24.86	30.30	31.67	29.97	27.50	8.29	3.69	tot	14.47	14.55
																		XMg	.15	.19

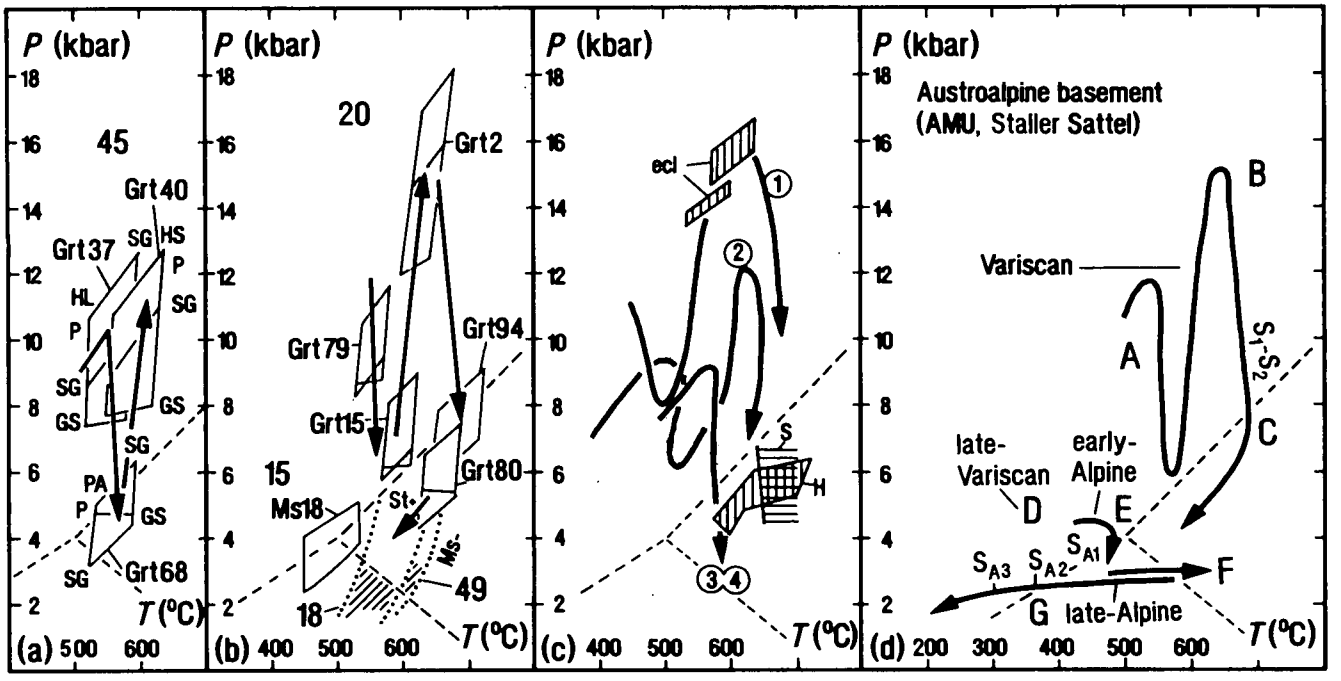

Text-Fig. 9.
P-T data and P-T paths from the Austroalpine basement to the south of the Tauern Window.

a,b) P-T data from samples 45, 20, 15, 18, 49 from the basement to the north of the Staller Sattel.
Numbers of P-T fields refer to analyses in Text-Figs. 5, 6, 8 and Table 1. Arrows connect the P-T fields in their temporal order. P-T field labelled Ms18 marks estimates from fine-grained muscovite in S_{A1}. P-T fields labelled 18 and 49 mark estimates for the thermal metamorphism in the Rieserferner contact aureole based on the petrogenetic grid of SPEAR & CHENEY (1989). See text for further explanation. Abbreviations of geothermo-barometers: GS = GHENT & STOUT (1981); HL = HOLDAWAY & LEE (1977); HS = HODGES & SPEAR (1982); P = PERCHUK et al. (1985); PA = PERCHUK & ARANOVITCH (1984); SG = GANGULY & SAXENA (1984).

c) P-T paths from micaschists of adjacent parts of the Austroalpine basement to the south of the Tauern Window, for comparison.
Encircled numbers refer to garnet zonation trends and locations in Text-Fig. 8h. ecl = P-T estimates from eclogitic amphibolites in the Prijakt area, Schobergruppe (SCHULZ, 1991; 1993); H = P-T estimates for the lower part of the MPU in the Kreuzeckgruppe (HOKE, 1990); S = P-T estimates for the upper part of the AMU in the Ahrn valley, Southern Tyrol (STÖCKHERT, 1985).

d) Synthesis of the pre-Alpine and Alpine structural and metamorphic evolution in the basement to the north of the Staller Sattel, compiled from a and b.
A = early prograde metamorphism; B = high-pressure eclogitic stage; C = high-temperature amphibolite-facies stage; D = intrusion of late-Variscan pegmatites; E = presumably early-Alpine overprinting; F = late-Alpine thermal metamorphism in the Rieserferner aureole; G = late-Alpine cooling during shear zone deformation along the DAV.

(Text-Fig. 9c, P-T path no. 1). Qualitative or geological errors arise from faulty assumption about equilibrium and crystal growth directions and cannot be easily assessed (SPEAR et al., 1990; HAUGERUD & ZEN, 1991). However, systematic errors do not affect the principal direction of the calculated P-T variations, as has been concluded by SPEAR & RUMBLE (1986) from garnet zonation profile simulation.

Further P-T estimates were obtained from muscovites of S_2-S_{A1} domains in sample 15. This sample shows no signs of a contact metamorphism. The compositions of the fine-grained muscovites (Text-Fig. 8m) signalize conditions around 450°C/3–4 kbar (CIPRIANI et al., 1971; VELDE, 1967; MASSONNE & SCHREYER, 1987) during formation of S_{A1} (Text-Fig. 9b).

Comparison of mineral parageneses with petrogenetic grids allows to bracket the conditions of the post-S_2 thermal metamorphism in the Rieserferner contact aureole. According to the petrogenetic grid for metapelites from SPEAR & CHENEY (1989), andalusite and staurolite stability fields intersect at 500 to 600°C/<3 kbar (Text-Fig. 9b) and give an estimate for conditions of crystallization of the assemblage andalusite + staurolite in samples 18, 19, 20 from the outer part of the contact aureole. Then occurrence of H_2O is considered, the assemblage Kfeldspar + sillimanite + muscovite + quartz in sample 49 near to the contact is stable in a divariant field which is bounded by the univariant curve of the muscovite-breakdown reaction (ALTHAUS et al., 1970) at high temperatures. A univariant sillimanite-andalusite transition curve signalizes corresponding minimum pressures of 2 kbars at these temperatures. Maximal pressures of 3 kbars are given by the andalusite and staurolite stability fields, and define a maximum temperature of 620°C in the inner part of the aureole (Text-Fig. 9b). Paragonitic compositions (high Na and low Si, Fe and Mg contents) of recrystallized white micas in S_{A1} domains of sample 20 (Text-Fig. 8l) confirm these low-pressure-high-temperature conditions of thermal metamorphism.

Biotite is not more stable in the fine-grained chlorite-muscovite-quartz-bearing S_{A2} domains of the phyllonites (e.g. in sample 15). This suggests temperatures below 400°C (YARDLEY, 1989) during development of this foliation. Temperatures around or slightly above 300°C (VOLL, 1976) in course of formation of S_{A3} can be derived from the plastically deformed quartz grains in the shear bands.

Summing up, the microstructural analysis of micaschists and phyllonites in combination with cation-exchange and net-transfer geothermobarometry, mineral chemistry of white micas and interpretation of mineral assemblages in petrogenetic grids, allowed to deduce a multistage metamorphic and tectonic history of the rocks between DAV and Rieserferner tonalite. An early prograde pre/syn-S_1 -S_2 metamorphism under high-pressure and subsequent high-temperature amphibolite-facies conditions was followed by a greenschist-facies stage with for-

mation of S_{A1}. Low-pressure-high-temperature conditions of thermal metamorphism in the Rieserferner contact aureole and later cooling are syn-S_{A2} and syn-S_{A3} events.

5. Pre-Alpine and Alpine Evolution

Several steps of deformation and metamorphism (A–G, Text-Fig. 9d) were preserved in garnet micaschists and chlorite-muscovite phyllonites of a small slice of basement to the north of the Staller Sattel. The evolution started with a successive development of foliations S_1 and S_2 by progressive deformation D_1-D_2 and a contemporaneous syndeformational prograde metamorphism with growth of garnet-bearing assemblages. These assemblages recorded increasing temperatures from 550°C (stage A) to 680°C and a significant variation of pressure, with a high-pressure stage (B) at 650°C/15 kbar and a subsequent high-temperature amphibolite-facies stage (C) at 680°C/7 kbar. Pegmatites intruded during probably late-Variscan times (stage D). The pegmatites and the earlier structures were overprinted by Alpine events. In a chlorite-muscovite phyllonite, the mineral chemistry of fine grained muscovite which underlines a foliation S_{A1} signalizes coeval greenschist-facies conditions of 450°C/3–4 kbar (stage E). Post-S_2 and post-S_{A1} andalusite + staurolite 2 and sillimanite + Kfeldspar + muscovite + quartz assemblages in some micaschists are related to a thermal metamorphism in the Rieserferner contact aureole. Temperatures of maximal 620°C at 2–3 kbar, estimated from petrogenetic grids, were reached next to the pluton (stage F). Subsequent cooling below 300°C, successive formation of steeply dipping S_{A2} and S_{A3} planes and a "phyllonitization" of the metapelites can be assigned to an upward directed sinistral strike-slip movement of the northern block along the Defereggen – Antholz – Vals shear zone (stage G).

Radiometric data from the small basement slice between DAV and Rieserferner tonalite is lacking. A temporal assignment of the single steps of deformation and metamorphism is only possible by lithological, structural and petrological comparison with dated rocks in adjacent parts of the basement. A pre-Alpine and post-Upper-Ordovician age of the stages A–C of the evolution (Text-Fig. 9d) can be concluded from several additional observations:

In the upper part of the metapsammopelite-amphibolite-marble unit (AMU), quartz-feldspar pegmatites with late-Variscan whole-rock Rb-Sr isochrons (Borsi et al., 1980; Hoke, 1990) cut across already foliated (S_2) and folded (F_3) host rocks (Stöckhert, 1984; 1987; Hoke, 1990) and signalize a pre-late-Variscan age of the structures. Garnet-bearing assemblages which recorded the high-pressure and subsequent amphibolite-facies stages of metamorphism of the micaschists to the north of the Staller Sattel are pre/syn-S_2. There, this foliation is as well cut by pegmatites, and therefore a late-Variscan minimum age of the metamorphism is probable.

Furthermore, as it has been outlined above, garnet compositional zonations reflect a history of continuous reactions depending on P and T of metamorphism. Consequently, garnet zonation trends and the derived P-T evolutions are characteristic properties of a geological unit. Similar garnet zonations as those in sample 20 and with the marked variation of Ca were recognized in micaschists of the Schobergruppe (Text-Fig. 8h, trend 1) and in the southern Deferegger Alps (Text-Fig. 8h, trend 2) of the lowermost parts of the metapsammopelitic unit (MPU), as well as in structurally upper parts (Text-Fig. 8i, trends 5 and 6) of the sequence (Schulz, 1990; 1992; 1993). Garnet zonations in sillimanite-biotite micaschists of the uppermost part of the underlying AMU unit resemble the trends observed from sample 45 (Text-Fig. 8h, trends 3 and 4; Schulz, unpublished data). P-T paths from all these micaschists display a similar marked decompression-compression as it can be derived from the samples to the north of the Staller Sattel (Text-Fig. 9c, d). A pre-late-Variscan minimum age of the P-T paths from the basement to the south of the DAV is indicated by the late-Variscan Rb-Sr mica isochrons in the southern block (Borsi et al., 1978) and can be presumed for the similar P-T evolution of the Staller Sattel samples.

Upper-Ordovician U-Pb zircon ages (Cliff, 1980) and Rb-Sr whole-rock isochrons (Borsi et al., 1973; Hammerschmidt, 1981) of pervasively sheared and foliated orthogneisses in the basement are interpreted to date the intrusion of former granitoids. The linear-planar structures of these orthogneisses are parallel to the foliation (S_2) and the lineation (L_2, Lcr_3) of the metapsammopelitic host rocks (Stöckhert, 1985; Schulz, 1988a; Huemer, 1991). This signalizes a post-Upper-Ordovician age of the deformation D_1-D_2 which produced the structures. Due to the syndeformational (D_1-D_2) growth of the garnet-bearing assemblages, the age of the metamorphism is post-Upper-Ordovician too.

A 30 Ma Rb-Sr whole rock isochron from the Rieserferner tonalite (Borsi et al., 1979) allows to fix a late-Alpine age of the thermal metamorphism in the contact aureole of the pluton. Formation of S_{A1} predates the growth of the contact metamorphic assemblages and could be early-Alpine. This is supported by early-Alpine (100 Ma) K-Ar muscovite ages from fine-grained muscovites in foliated late-Variscan pegmatites (Stöckhert, 1984, 1987). The ductile deformation along the Defereggen – Antholz – Vals line (DAV) with development of the foliations S_{A2} and S_{A3} started contemporaneously with the Rieserferner intrusion as is indicated by a syncrystalline rotation of contact metamorphic porphyroblasts, and progressed during decreasing temperatures. When Rb-Sr biotite ages are interpreted to date the cooling below 300±50°C (Jäger, 1979), isochrons from biotites in the southern parts of the northern block (Borsi et al., 1978) suggest an age of 28 Ma for the formation of the foliation S_{A3}.

That way, detailed study of metapelites which bear structural domains with preserved microstructures, mineral assemblages and mineral chemistry of earlier stages of metamorphism and deformation, provides considerable insight into the tectono-metamorphic evolution of crystalline terranes.

Acknowledgements

The Michelitsch family in Erlsbach supported the field work in the Deferegger Alps during several years. Microprobe analyses at Mineralogisches und Petrologisches Institut der Universität Bonn were assisted by B. Spiering; A. Peterek (Erlangen) helped to interpret structural data. G. Nollau (Erlangen), C. Triboulet (Paris) and P. Göbel generously checked the manuscript. The work was financed by a grant (Schu 676/2) from the Deutsche Forschungsgemeinschaft DFG.

References

ALTHAUS, E., KAROTKE, E., NITSCH, K.H. & WINKLER, H.G.F.: An experimental re-examination of the upper stability limit of muscovite plus quartz. – N. Jb. Min. Mh., 1970, H. **7**, 325–336, Stuttgart 1970.

ANGELIER, J. & MECHLER, P.: Sur une méthode graphique de recherche des contraintes principales également utilisable en tectonique et en séismologie: la méthode des dièdres droits. – Bull. Soc. géol. France, **29**, 1309–1318, Paris 1977.

ASHWORTH, J.R. & EVIRGEN, M.M.: Plagioclase relations in pelites, central Menderes Massif, Turkey. I. The peristerite gap with coexisting kyanite. – J. metamorphic Geol., **3**, 207–218, Oxford 1985a.

ASHWORTH, J.R. & EVIRGEN, M.M.: Plagioclase relations in pelites, central Menderes Massif, Turkey. II. Perturbation of garnet-plagioclase geobarometers. – J. metamorphic Geol., **3**, 219–230, Oxford 1985b.

BECKE, F.: Petrographische Studien am Tonalit des Rieserferner. – Tschermaks Min. Petr. Mitt., **13**, 379–433, Wien 1892.

BEHRMANN, J.H. & PLATT, J.P.: Sense of nappe emplacement from quartz c-axis fabrics; an example from the Betic Cordilleras (Spain). – Earth and Planet. Sci. Lett., **59**, 208–215, Oxford 1982.

BELL, T.H., RUBENACH, M.J. & FLEMING, P.D.: Porphyroblast nucleation, growth and dissolution in regional metamorphic rocks as a function of deformation partitioning during foliation development. – J. metamorphic Geol., **4**, 37–67, Oxford, 1986.

BELLIENI, G. & VISONA, D.: Metamorphic evolution of the Austroalpine schists outcropping between the intrusive masses of Vedrette di Ries and Cima di Vila, Eastern Alps, Italy. – N. Jb. Geol. Paläont., Mh., **1981**, 586–602, Stuttgart 1981.

BORSI, S., DEL MORO, A., SASSI, F.P., VISONA, D. & ZIRPOLI, G.: On the existence of Hercynian aplites and pegmatites in the lower Aurina Valley (Ahrntal, Austrides, Eastern Alps). – N. Jb. Min. Mh., **1980**, 501–514, Stuttgart 1980.

BORSI, S., DEL MORO, A., SASSI, F.P. & ZIRPOLI, G.: Metamorphic evolution of the Austridic rocks to the south of the Tauern Window (Eastern Alps): radiometric and geopetrologic data. – Mem. Soc. Geol. Ital., **12**, 549–571, Rom 1973.

BORSI, S., DEL MORO, A., SASSI, F.P., ZANFERRARI, A. & ZIRPOLI, G.: New geopetrologic and radiometric data on the Alpine history of the Austridic continental margin south of the Tauern Window. – Mem. Ist. Geol. Min. Univ. Padova, **32**, 1–17, Padova 1978.

BORSI, S., DEL MORO, A., SASSI, F.P. & ZIRPOLI, G.: On the age of the Vedrette de Ries (Rieserferner) massif and its geodynamic significance. – Geol. Rdsch., **68**, 41–60, Stuttgart 1979.

BOUCHEZ, J.L. & PECHER, A.: The Himalayan Main Central Thrust pile and its quartz-rich tectonites in Central Nepal. – Tectonophysics, **78**, 23–50, Amsterdam 1981.

CARMICHAEL, D.M.: On the mechanism of prograde metamorphic reactions in quartz-bearing pelitic rocks. – Contrib. Mineral. Petrol., **20**, 244–267, Heidelberg 1969.

CESARE, B.: Metamorphismo di contatto di rocce pelitiche nell'aureola di Vedrette di Ries (Alpi Orientali – Italia). – Thesis Università di Padova (unpubl.), 105 S., Padova 1991.

CIPRIANI, C., SASSI, F.P. & SCOLARI, A.: Metamorphic white micas: definition of paragenetic fields. – Schweiz. Mineral. Petrogr. Mitt., **51**, 259–302, Zürich 1971.

CLIFF, R.A.: U-Pb isotopic evidence from zircons for lower Palaeozoic tectonic activity in the Austroalpine nappe, the Eastern Alps. – Contrib. Mineral. Petrol., **71**, 283–288, Heidelberg 1980.

FROST, B.R. & TRACY, R.J.: P-T paths from zoned garnets: some minimum criteria. – Am. J. Sci., **291**, 917–939, New Haven, 1991.

GANGULY, J. & SAXENA, S.K.: Mixing properties of aluminosilicate garnets: constraints from natural and experimental data, and applications to geothermo-barometry. – Amer. Mineral., **69**, 88–97, Ann Arbor, 1984.

GHENT, E.D. & STOUT, M.Z.: Geobarometry and geothermometry of plagioclase-biotite-garnet-muscovite assemblages. – Contrib. Mineral. Petrol., **76**, 92–97, Heidelberg 1981.

GRUNDMANN, G. & MORTEANI, G.: The young uplift and thermal history of the central Eastern Alps (Austria/Italy), evidence from apatite fission track ages. – Jb. Geol. B.-A., **128**, 197–216, Wien 1985.

HAMMERSCHMIDT, K.: Isotopengeologische Untersuchungen am Augengneis Typ Campo Tures bei Rain in Taufers, Südtirol. – Mem. Ist. Geol. Min. Univ. Padova, **34**, 273–300, Padova 1981.

HAUGERUD, R.A. & ZEN, E.A.: An essay on metamorphic path studies or Cassandra in P-T- space. – In: PERCHUK, L.L. (Ed.): Progress in metamorphic and magmatic petrology, 323–348, Cambridge (Cambridge University Press) 1991.

HODGES, K.V. & SPEAR, F.S.: Geothermometry, geobarometry and the Al_2SiO_5 triple point at Mt. Moosilauke, New Hampshire. – Amer. Mineral., **67**, 1118–1134, Ann Arbor 1982.

HOFMANN, K.H., KLEINSCHRODT, R., LIPPERT, R., MAGER, D. & STÖCKHERT, B.: Geologische Karte des Altkristallins südlich des Tauernfensters zwischen Pfunderer Tal und Tauferer Tal (Südtirol). – Der Schlern, **57**, 572–590, Bozen 1983.

HOKE, L.: The Altkristallin of the Kreuzeck Mountains, SE Tauern Window, Eastern Alps – basement crust in a convergent plate boundary zone. – Jb. Geol. B.-A., **133**, 5–87, Wien 1990.

HOLDAWAY, M.J. & LEE, S.M.: Fe-Mg cordierite stability in high-grade pelitic rocks based on experimental, theoretical and natural observations. – Contrib. Mineral. Petrol., **63**, 175–198, Heidelberg 1977.

HUEMER, T.: Kartierung, Strukturgeologie und Petrographie im Altkristallin südlich von Antholz (Westliche Deferegger Alpen, Südtirol, Italien). – Diplomarbeit Institut für Geologie und Mineralogie der Universität Erlangen-Nürnberg (unpubl.), 101 S., Erlangen 1991.

JÄGER, E.: The Rb-Sr method. – In: JÄGER, E. & HUNZIKER, J.C. (Eds.): Lectures in Isotope Geology, 13–26, Berlin (Springer) 1979.

KLEINSCHRODT, R.: Quarzkorngefügeanalyse im Altkristallin südlich des westlichen Tauernfensters (Südtirol/Italien). – Erlanger geol. Abh., **114**, 1–82, Erlangen 1987.

KOZIOL, A.M. & NEWTON, R.C.: Redetermination of the anorthite breakdown reaction and improvement of the plagioclase-garnet-Al_2SiO_5-quartz geobarometer. – Amer. Mineral., **73**, 216–223, Ann Arbor 1988.

LISTER, G.S. & HOBBS, B.E.: The simulation of fabric development during plastic deformation and its application to quartzite: the influence of the deformation history. – J. Struct. Geol., **2**, 335–370, Oxford 1980.

MAGER, D.: Geologische und petrographische Untersuchungen am Südrand des Rieserferner-Plutons (Südtirol) unter Berücksichtigung des Intrusionsmechanismus. – Dissertation Naturwissenschaftliche Fakultät der Universität Erlangen-Nürnberg (unpubl.), 182 S., Erlangen 1985.

MARTIGNOLE, J. & NANTEL, S.: Geothermobarometry of cordierite-bearing metapelites near the Morin anorthosite complex, Grenville province, Quebec. – Canad. Mineral., **20**, 307–318, Ontario 1982.

MASSONNE, H.-J. & SCHREYER, W.: Phengite geobarometry based on the limiting assemblage with K-feldspar, phlogopite and quartz. – Contrib. Mineral. Petrol., **96**, 212–224, Heidelberg 1987.

NEWTON, R.C. & HASELTON, H.T.: Thermodynamics of the garnet-plagioclase-Al_2SiO_5-quartz geobarometer. – In: NEWTON, R.C., NAVROTSKY, A. & WOOD, B.J. (Eds.): Thermodynamics of minerals and melts, 131–147, New York (Springer) 1981.

PERCHUK, L.L. & ARANOVITCH, L.Y.: Improvement of garnet-biotite geothermometer: correction for fluorine content in biotite. – Dokl. Acad. Sci. USSR, **277**, 471–475, Moskau 1984.

PROCHASKA, W.: Die Rieserfernerintrusion und ihre Kontaktaureole. – Fortschr. Mineral. Bh., **59**, H. 2, 118–125, Berlin 1981a.
PROCHASKA, W.: Einige Ganggesteine der Rieserfernerintrusion mit neuen radiometrischen Altersdaten. – Mitt. Ges. Geol. Bergbaustud. Österr., **27**, 161–171, Wien 1981b.

SCHMIDEGG, O.: Steilachsige Tektonik und Schlingenbau auf der Südseite der Tiroler Zentralalpen. – Jb. Geol. B.-A., **86**, 115–149, Wien 1936.
SCHULZ, B.: Deformation und Metamorphose im ostalpinen Altkristallin südlich des Tauernfensters (südliche Deferegger Alpen, Österreich). – Schweiz. Mineral. Petrogr. Mitt., **68**, 397–406, Zürich 1988a.
SCHULZ, B.: Quarz- und Mikrogefüge zonierter Kalksilikatgneis-Körper im ostalpinen Altkristallin (südliche Deferegger Alpen, Österreich). – Erlanger geol. Abh., **116**, 117–122, Erlangen 1988b.

SCHULZ, B.: Jungalpidische Gefügeentwicklung entlang der Defereggen-Antholz-Vals-Linie (Osttirol, Österreich). – Jb. Geol. B.-A., **132**, 775–789, Wien 1989.
SCHULZ, B.: Prograde-retrograde P-T-t-deformation path of Austroalpine micaschists during Variscan continental collision (Eastern Alps). – J. metamorphic Geol., **8**, 629–642, Oxford 1990.
SCHULZ, B.: Mineralchemie in Eklogit-Amphiboliten und Glimmerschiefern der Schobergruppe und frühvariskische Hochdruckmetamorphose im ostalpinen Basement südlich des Tauernfensters. – Nachr. Dt. Geol. Ges., **46**, S. 62, Hannover 1991.
SCHULZ, B.: Pre-Alpine high-pressure metamorphism in the Austroalpine basement: P-T-t-deformation paths from samples to the south of the Tauern Window. – Zbl. Geol. Paläont. Teil I, 1992 **(1/2)**, 93–103, Stuttgart 1992.
SCHULZ, B.: Mineral chemistry, geothermobarometry and pre-Alpine high-pressure metamorphism of eclogitic amphibolites and mica schists from the Schobergruppe, Austroalpine basement, Eastern Alps. – Mineral. Mag., 189–202, London 1993.
SCHULZ, B., NOLLAU, G., HEINISCH, H. & GODIZART, G.: Austroalpine basement complex to the south of the Tauern Window. – In: VON RAUMER, J.F. & NEUBAUER, F. (Eds.): The pre-Mesozoic Geology in the Alps, 495–514, Heidelberg (Springer) 1993.
SENARCLENS-GRANCY, W.: Beiträge zur Geologie der Deferegger Berge und der westlichen Schobergruppe in Osttirol. – Cbl. f. Min. Geol. Paläont. Abt. B Abh., 1932, 481–490, Stuttgart 1932.

SENARCLENS-GRANCY, W.: Zur Grundgebirgs- und Quartärgeologie der Deferegger Alpen und ihrer Umgebung. – Z. dt. geol. Ges., **116**, 502–511, Hannover 1964.
SENARCLENS-GRANCY, W.: Geologische Karte der westlichen Deferegger Alpen 1 : 25 000. – Geol. B.-A. Österreich (Ed.), Wien 1972.
SPEAR, F.S.: On the interpretation of peak metamorphic temperatures in light of garnet diffusion during cooling. – J. metamorphic Geol., **9**, 379–388, Oxford 1991.
SPEAR, F.S. & CHENEY, J.T.: A petrogenetic grid for pelitic schists in the system SiO_2 – Al_2O_3 – FeO – MgO – K_2O – H_2O. – Contrib. Mineral. Petrol., **101**, 149–164, Heidelberg 1989.
SPEAR, F.S. & RUMBLE, D.: Pressure, temperature and structural evolution of the Orfordville Belt, West-Central New Hampshire. – J. Petrol., **27**, 1071–1093, Oxford 1986.
SPEAR, F.S. & SELVERSTONE, J.: Quantitative P-T paths from zoned minerals: theory and tectonic applications. – Contrib. Mineral. Petrol., **83**, 348–357, Heidelberg 1983.
SPEAR, F.S., SELVERSTONE, J., HICKMOTT, D., CROWLEY, P. & HODGES, K.V.: P-T paths from garnet zoning: a new technique for deciphering tectonic processes in crystalline terranes. – Geology, **12**, 87–90, Boulder 1984.
SPEAR, F.S., KOHN, M.J., FLORENCE, F.P. & MENARD, T.: A model for garnet and plagioclase growth in pelitic schists: implications for thermometry and P-T path determinations. – J. metamorphic Geol., **8**, 683–696, Oxford 1990.
SPRY, A.: Metamorphic textures. – 350 S., Oxford (Pergamon Press) 1969.
STÖCKHERT, B.: K-Ar determinations on muscovites and phengites and the minimum age of the Old Alpine deformation in the Austridic basement south of the Tauern Window (Ahrn valley, Southern Tyrol, Eastern Alps). – N. Jb. Min. Abh., **150**, 103–120, Stuttgart 1984.
STÖCKHERT, B.: Pre-Alpine history of the Austridic basement to the south of the western Tauern Window (Southern Tyrol, Italy) – Caledonian versus Hercynian event. – N. Jb. Geol. Paläont. Mh., 1985 **(10)**, 618–642, Stuttgart 1985.
STÖCKHERT, B.: Das Uttenheimer Pegmatit-Feld (Ostalpines Altkristallin, Südtirol). Genese und alpine Überprägung. – Erlanger geol. Abh., **114**, 83–106, Erlangen 1987.
ST-ONGE, M.R.: Zoned poikiloblastic garnets: P-T paths and syn-metamorphic uplift through 30 km of structural depth, Wopmay orogen, Canada. – J. Petrol., **28**, 1–21, Oxford 1987.

THOMPSON, A.B.: Mineral reactions in pelitic rocks. – Am. J. Sci., 276, 401–454, New Haven 1976.
TRACY, R.J.: Compositional zoning and inclusions in metamorphic minerals. – In: FERRY, J.M. (Ed.): Characterization of metamorphism through mineral equilibria, Reviews in Mineralogy, **10**, 355–397, Min. Soc. Am. 1982.
TRIBOULET, C. & AUDREN, C.: Continuous reactions between biotite, garnet, staurolite, kyanite/sillimanite/andalusite and P-T-time deformation path in the micaschists from the estuary of the River Vilaine, South Brittany, France. – J. metamorphic Geol., **3**, 91–105, Oxford 1985.
TRZCIENSKI, W.E.: Garnet zoning – product of a continuous reaction. – Canad. Mineral., **15**, 250–256, Ontario 1977.

VELDE, B.: Si^{4+} contents of natural phengites. – Contrib. Mineral. Petrol., **14**, 250–258, Heidelberg 1967.
VERNON, R.H.: Porphyroblast-matrix microstructural relationships in deformed metamorphic rocks. – Geol. Rdsch., **67**, 288–305, Stuttgart 1978.
VOLL, G.: Klastische Mineralien aus den Sedimentserien der Schottischen Highlands und ihr Schicksal bei aufsteigender Regional- und Kontaktmetamorphose. – Habilitationsschrift Fakultät für Bergbau und Hüttenwesen der Technischen Universität Berlin, D 83, 1–360, Berlin 1968.
VOLL, G.: Recrystallization of quartz, biotite and feldspars from Erstfeld to the Leventina Nappe, Swiss Alps, and its geological significance. – Schweiz. Mineral. Petrogr. Mitt., **56**, 641–647, Zürich 1976.

YARDLEY, B.W.D.: An introduction to metamorphic petrology. – 248 S., Essex (Longman) 1989.

ZARSKE, G.: Kartierung, Strukturgeologie und Petrographie im Altkristallin zwischen Erlsbach und Oberseitsee in den nordwestlichen Deferegger Alpen, Osttirol. – Diplomarbeit Institut für Geologie und Paläontologie der Techn. Universität Clausthal (unpubl.), 178 S., Clausthal 1985.

Manuskript bei der Schriftleitung eingelangt am 15. Oktober 1992